Aus dem Department für Biomedizinische Wissenschaften

der Veterinärmedizinischen Universität Wien

Institut für Tierzucht und Genetik

(Leiter: O.Univ.-Prof. Dr.med.vet. Mathias Müller)

Effects of growth hormone receptor deficiency on the hypothalamus pituitary axis: alterations in feedback mechanisms and metabolism-associated signaling pathways

Diplomarbeit

Veterinärmedizinische Universität Wien

vorgelegt von

Martin Kraetzl

Wien, im Februar 2021

Betreuer: O.Univ.-Prof. Dr.med.vet. Mathias Müller
Institut für Tierzucht und Genetik
Department für Biomedizinische Wissenschaften
Veterinärmedizinische Universität Wien

Externe Betreuer: Prof. Dr.med.vet. Eckhard Wolf
und Dr.med.vet. Arne Hinrichs
Lehrstuhl für Molekulare Tierzucht und Biotechnologie
Veterinärwissenschaftliches Department
Tierärztliche Fakultät
Ludwig-Maximilians-Universität München

Begutachter: Univ.-Prof. Dr.med.vet. Maik Dahlhoff
Institut für In-vivo und In-vitro-Modelle
Department für Biomedizinische Wissenschaften
Veterinärmedizinische Universität Wien

Table of contents

Für meine Eltern

1. Introduction

The hypothalamus pituitary axis (HP axis) is the central part of the endocrine control of growth, metabolism and reproduction under the control of complex regulatory feedback mechanisms.

In the last decades, the development of animal models with genetic manipulations in growth hormone (GH)-related signaling cascades allowed deep insight into physiological and pathophysiological principles of growth and the associated metabolism (Kopchick 2003, Kopchick et al. 1999). Models for Laron syndrome (LS), a syndrome caused by growth hormone receptor deficiency (GHRD), revealed new insights into the role of GH and insulin-like growth factor 1 (IGF1) in physiological and pathophysiological processes.

Individuals with GHRD display low levels of circulating IGF1 while GH levels are constantly elevated. This leads to a complex phenotype including postnatal growth retardation and juvenile hypoglycemia (Laron and Kopchick 2011). Astonishingly, while an increased accumulation of body fat is associated with GHRD, a protective effect against the development of malignancies such as diabetes and cancer is described (Basu et al. 2018). This leads to questions of mechanisms modulating energy homeostasis within GHRD individuals.

The hypothalamus is a key unit of this homeostatic regulation of energy balance and metabolism via anorexigenic and orexigenic signals like 5' adenosine monophosphate-activated protein kinase (AMPK) (Hardie et al. 2012) and mechanistic target of rapamycin (mTOR) (Cota et al. 2006). Together with the anterior pituitary gland, it is part of the HP axis and its complex feedback mechanisms, controlling GH and IGF1 levels in the circulation (Varela-Nieto and Chowen 2005). Thus, these organs play a major role in the pathophysiology of GHRD and the resulting metabolism.

The aim of this thesis was to investigate the disturbances in regulatory feedback mechanisms associated with constantly high serum GH and low IGF1 levels. Furthermore, we wanted to clarify, whether alterations in hypothalamic leptin signaling mediate the altered metabolic phenotype in GHRD.

Therefore, we examined total abundance and phosphorylation status of GH- and metabolism-related hypothalamic and anterior pituitary signaling molecules in a porcine model for LS (Hinrichs et al. 2018).

2. Review of the literature

2.1. The hypothalamus as an endocrine control center

The hypothalamus is a key regulator of somatic, vegetative and metabolic processes. For energy homeostasis, especially the arcuate nucleus (ARC) and its neurons play an important role by expressing the orexigenic neuropeptide Y (NPY) and agouti-related peptide (AGRP) as well as the anorexigenic proopiomelanocortin (POMC). Influenced by hormonal and nutritional stimuli, like blood glucose, insulin, and leptin from the circulation, these neurons transduce their signals to a variety of other hypothalamic regions, like the paraventricular hypothalamic nucleus (PVN), the lateral hypothalamus (LHT), the ventromedial hypothalamus (VMN), and the dorsomedial hypothalamus (DMH). The interplay of these neurons with external stimuli leads to a complex response to the current body energy status as well as the regulation of food intake and energy expenditure (Kleinridders et al. 2009, Roh and Kim 2016, Waterson and Horvath 2015).

Additionally, the hypothalamus is an important player in the endocrine regulation of a broad spectrum of processes, like metabolism, reproduction, and growth. The foundation for these processes is a complex pulsatile interaction between the central hypothalamic signal and the subordinated pituitary gland, called HP axis.

Hypothalamic signals reach the pituitary gland in two different ways. On the one hand, hypothalamic antidiuretic hormone (ADH; synonymous vasopressin) and oxytocin are transported intracellularly via axons from the paraventricular and supraoptic hypothalamic nuclei to the posterior pituitary gland, were they are stored and released (Leng et al. 2015). On the other hand, the hypothalamic hormones gonadotropin-releasing hormone (GNRH), corticotropin-releasing hormone (CRH), thyrotropin-releasing hormone (TRH), somatostatin (SST; synonymous somatotropin release-inhibiting hormone/SRIH) and growth hormone-releasing hormone (GHRH; synonymous somatoliberin) reach the anterior pituitary gland via the hypophyseal portal system. These hypothalamic releasing or inhibiting hormones stimulate or inhibit the production and release of the anterior pituitary hormones luteinizing hormone (LH)

and follicle stimulating hormone (FSH), adrenocorticotropin (ACTH), thyroid-stimulating hormone (TSH), prolactin, and GH (synonymous somatotropin) (Clarke 2015, Cocco et al. 2017, Keenan and Veldhuis 2016, Sam and Frohman 2008).

Hypothalamic signaling and its action via the HP axis consist of a tremendous number of neuronal, metabolic and endocrine stimuli from the central nervous system and the periphery that in detail still remain partly unclear.

2.2. The somatotropic axis

GH secretion from somatotropic cells in the anterior pituitary gland is regulated by a variety of signals. While hypothalamic SST has an inhibiting effect, GHRH stimulates the secretion of GH into the circulation (Giustina and Veldhuis 1998). Its effects are displayed in a variety of tissues directly by GH or via IGF1. Besides other tissues where GH-induced IGF1 conveys its effects on growth and metabolism in a paracrine and autocrine manner, liver derived IGF1 acts as an important endocrine signal in the organism (Varela-Nieto and Chowen 2005).

Negative feedback of IGF1 as well as GH itself inhibits GH-stimulatory signaling in the hypothalamus, but also directly in the anterior pituitary gland (Asa et al. 2000, Peng et al. 2001). The underlying signaling cascades for negative IFG1 feedback remain unclear (Romero et al. 2010).

Besides this classical hypothalamus-pituitary interplay, a variety of other central and peripheral signals are also relevant for the regulation of the somatotropic axis. They range from other neuropeptides, like substance P, TRH, galanin, calcitonin, and NPY, over hormones like glucocorticoids, sex hormones, thyroid hormones, insulin, and leptin, to metabolites, like free fatty acids (FFA), glucose, and amino acids (Giustina and Veldhuis 1998). These influences lead to the versatile regulation of pulsatile GH secretion (Keenan and Veldhuis 2016) and illustrate the complex regulation of the somatotropic axis (**Figure 1**).

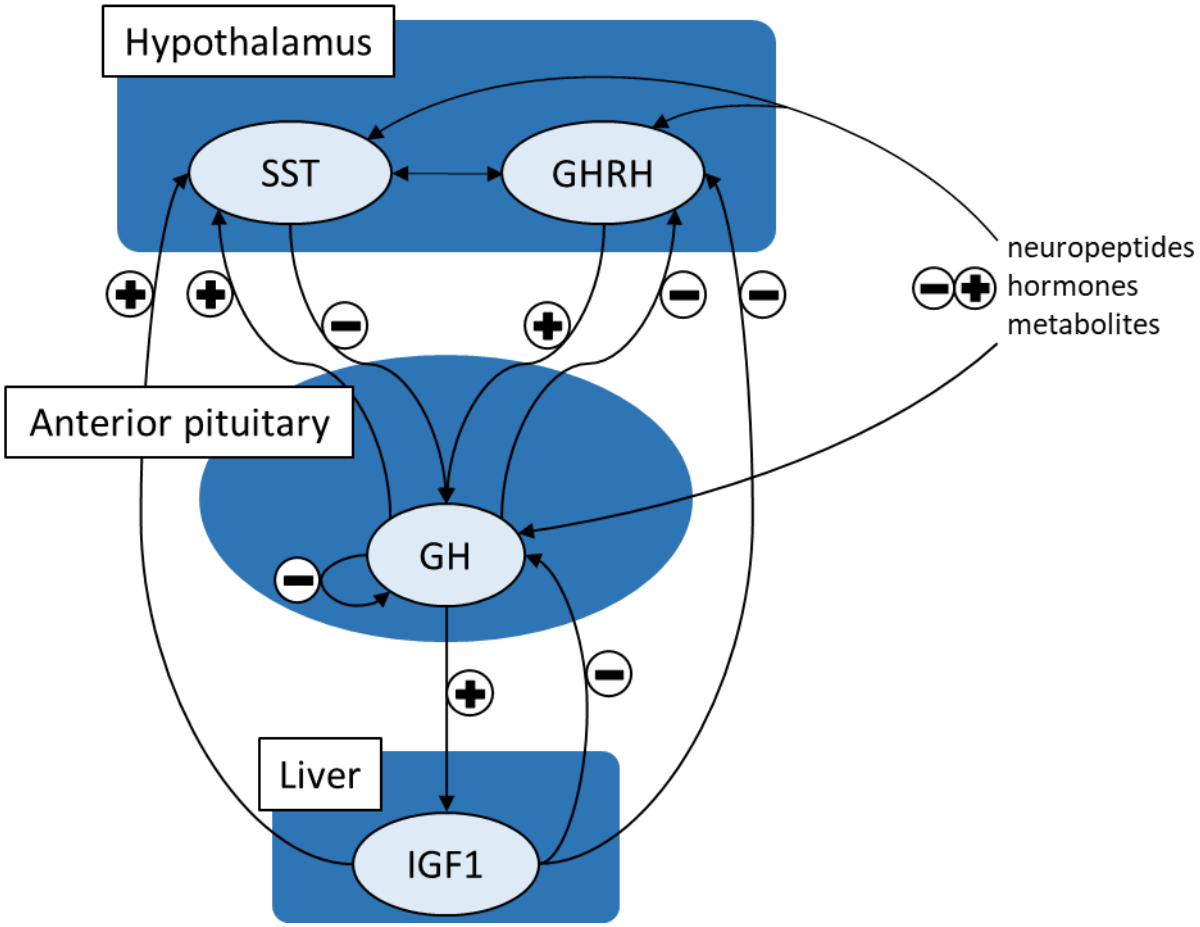

Figure 1. Schematics of regulatory loops of the somatotropic axis in hypothalamus, anterior pituitary and liver. Arrows with plus denote positive effector pathways, whereas arrows with minus represent negative feedback. Abbreviations: growth hormone (GH), growth hormone-releasing hormone (GHRH), insulin-like growth factor 1 (IGF1), somatostatin (SST) (adapted from Giustina et al. (Giustina and Veldhuis 1998)).

The pulsatile GH signal can act directly via the growth hormone receptor (GHR), but mostly operates via the production of IGF1 in the liver (Kaplan and Cohen 2007). IGF1 and its receptor (IGF1R) share a high degree of homology with insulin and insulin receptor (INSR) (Laron 2004, Pedrini et al. 1994). Heterodimeric receptors have different effects as typical homodimeric receptors, but use the same intracellular signaling cascade via insulin receptor substrate 1 (IRS1) and can assemble to INSR/IGF1R-hybrids (Bailyes et al. 1997, Copps and White 2012, Laviola et al. 2007, Pandini et al. 2002).

For the regulation of IGF1 effects, IGF binding proteins (IGFBPs) are especially important as serum carriers. Due to their affinity to IGF1 they extend its serum half-life,

regulate tissue distribution and in most circumstances inhibit IGF1 effects (Bach 2018, Rajaram et al. 1997).

Outcomes of upregulated growth hormone/insulin-like growth factor axis can be split into anabolic and catabolic ones. Anabolic effects like ribonucleic acid and protein synthesis lead to cell proliferation and differentiation in various tissues and consequently to processes like muscle growth and longitudinal bone growth. In addition, antiapoptotic effects of IGF1 are described. On the other hand, catabolic effects like lipid degradation to FFA and glycerol, antagonistic compared to insulin, also represent effects of the GH/IGF1 axis (Bergan-Roller and Sheridan 2018, Isaksson et al. 1987, Laviola et al. 2007).

Alterations in this system can lead to severe disorders regarding metabolism, maturation, and growth. GHRD for example leads to dwarfism and severe obesity (Laron 2008, Laron et al. 2017).

2.3. Leptin and adiposity

Leptin is an adipose tissue-derived proteohormone, discovered by Friedmann et al. (Zhang et al. 1994), produced by the expression of the obese gene (*OB*/*LEP*, OMIM#164160) (Masuzaki et al. 1995).

It plays a major role in the suppression of food intake and the stimulation of energy expenditure (Friedman and Halaas 1998, Myers et al. 2008). Circulating leptin serves as a signal for body energy stored in white adipose tissue and is highly correlated with body fat percentage and body mass index (BMI) (Considine et al. 1996, Maffei et al. 1995, Rosenbaum et al. 1996).

To convey its effect, leptin passes the blood-brain barrier (BBB) (Banks et al. 1996) and mostly binds to the long-form leptin receptor (LRb) (Myers et al. 2008). LRb is strongly expressed in different hypothalamic nuclei, like ARC, PVN, LHT, VMN, and DMH, that are involved in the regulation of food intake and body weight (Fei et al. 1997, Mercer et al. 1996).

Leptin binding to its receptor activates downstream signaling via phosphorylation of janus kinase (JAK) and signal transducer and activator of transcription (STAT3) (Bates SH et al. 2003) and consequently upregulates the transcription of the anorexigenic neuropeptide POMC and decreases transcription of orexigenic NPY and AGRP (Gao et al. 2004, Kwon et al. 2016, Park and Ahima 2014).

Similar to the insulin receptor, the leptin receptor (LEPR) signaling cascade also acts via IRS1-phosphoinositide 3-kinase (PI3K)-protein kinase B (AKT) pathway in the hypothalamus (Niswender and Schwartz 2003) and regulates transcription of POMC and AGRP via forkhead box protein O1 (FOXO1) (Kwon et al. 2016, Park and Ahima 2014).

mTOR complex 1 (mTORC1) (Cota et al. 2006) and AMPK (Minokoshi et al. 2004) are described as leptin regulated targets in the hypothalamic regulation of food intake. While fasting activates hypothalamic AMPK by phosphorylation of its catalytic α-subunit (threonine 172), refeeding and high serum leptin levels inhibit AMPK, leading to reduced food intake and body weight (Minokoshi et al. 2004). By way of contrast, leptin activates signaling of mTOR/ribosomal protein S6 kinase (S6K) via PI3K-AKT to display its anorexigenic effect. An activation of mTOR/S6K also leads to an inactivation of AMPK linking these regulatory pathways (Kwon et al. 2016, Park and Ahima 2014). A schematic summary of the AMPK/mTOR interplay is provided in **Figure 2**.

Malfunction in these regulatory cascades can lead to severe metabolic disorders. In obesity, for example, permanently elevated serum leptin levels from excessive adipose tissue can lead to a decreased leptin effect on appetite and body weight due to decreased leptin access to the brain and/or cellular leptin insensitivity in hypothalamic neurons and consequently leptin resistance (Cui et al. 2017, El-Haschimi et al. 2000, Liu et al. 2018). Possible players in leptin resistance in general are disorders of leptin transport via the BBB, competitive inhibition by circulating leptin-binding proteins, divers mutations of the leptin receptor gene, and inhibition of intracellular leptin signaling molecules such as STAT3 (Kwon et al. 2016, Liu et al. 2018).

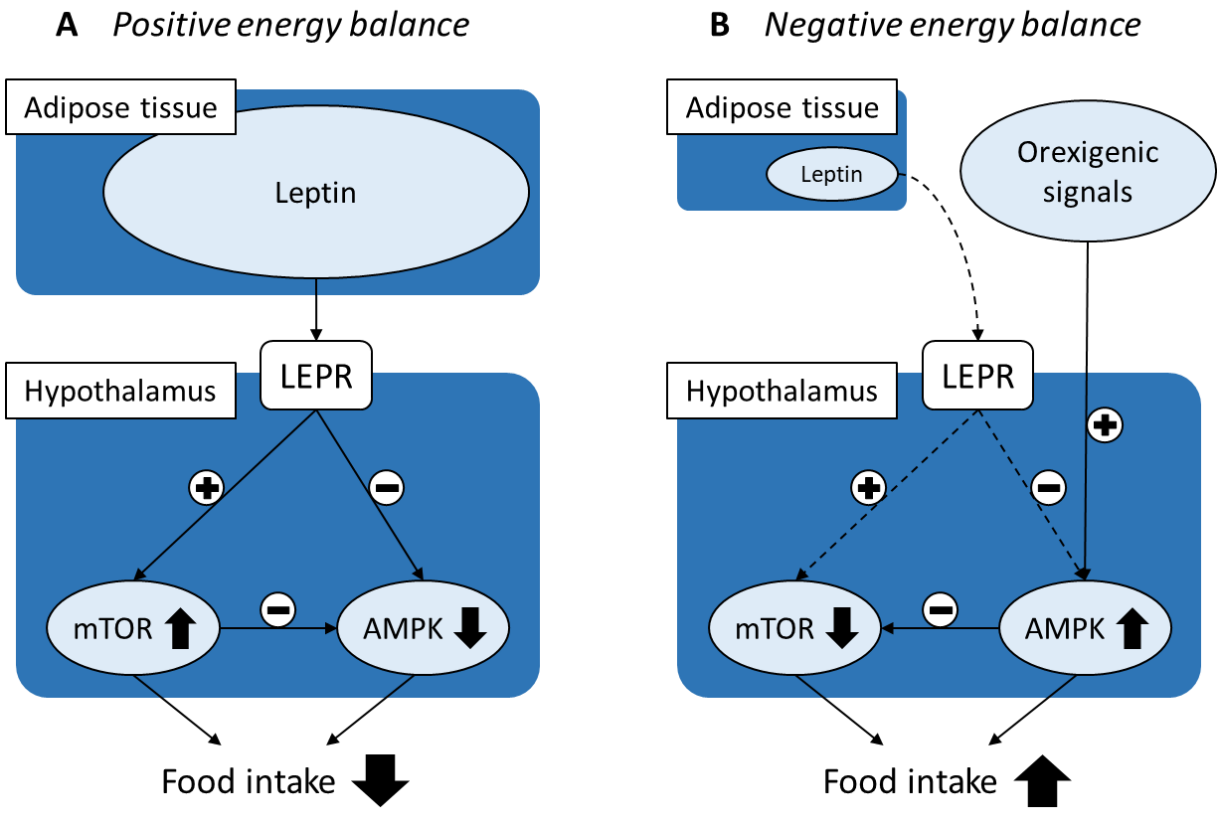

*Figure 2. Schematics of hypothalamic regulation of food intake by leptin via anorexigenic mTOR and orexigenic AMPK. **A**: state of high fuel / high body energy stores. **B**: state of low fuel / caloric restriction. Arrows with plus denote activation, whereas arrows with minus represent inhibition. Dashed lines illustrate lower signaling activity. Abbreviations: 5' adenosine monophosphate-activated protein kinase (AMPK), leptin receptor (LEPR) and mechanistic target of rapamycin (mTOR).*

2.4. The human Laron syndrome

The clinical phenotype of LS, or primary growth hormone insensitivity (OMIM#262500), was discovered by Laron et al. in 1966 (Laron et al. 1966).

It is a very rare autosomal recessive hereditary disorder caused by different mutations of the growth hormone receptor gene (*GHR*) causing GHRD. While patients with genetic background from the Middle East, referred to as *Israeli cohort*, have different mutations of the *GHR* and thus show different phenotypes, a quite homogenous cohort in Ecuador was found (*Ecuadorian cohort*), mostly carrying the E180 splice mutation (Amselem et al. 1989, Godowski et al. 1989, Rosenbloom and Guevara-Aguirre 1998, Rosenfeld et al. 1994).

In homozygous individuals, these loss-of-function mutations principally lead to deficient GH action in various tissues, affecting nearly the whole organism. This also leads to a lack of GH stimulated production of IGF1 in the liver and therefore distinctly reduced serum IGF1 levels. Due to the lost negative feedback of IGF1 in the anterior pituitary gland and the hypothalamus, the plasma GH is increased (Eshet et al. 1984, Laron and Klinger 1994, Varela-Nieto and Chowen 2005).

These effects of GHRD lead to a variety of pathological phenomena in patients with LS. The phenotype of LS is mainly presented by dwarfism, underdevelopement of the facial bones, crowded and defective teeth, obesity, acromicria, organomicria, delayed puberty and juvenile hypoglycemia (Laron and Kopchick 2011). While birthweight is normal, retarded growth can be seen during infancy leading to dwarfism in adults (Laron and Kopchick 2011).This can be explained by GH independent embryonic growth, but postnatal growth is dependent on GH-IGF1 axis (Baker et al. 1993, Hetz et al. 2015, Le Roith et al. 2001).

Lost lipolytic effects of GH in adipose tissue lead to severe obesity. Compared to BMI-matched obese people without GHRD, leptin levels are lower in the *Ecuadorian cohort,* suggesting a protective effect of GHRD against leptin resistance (Guevara-Aguirre et al. 2015).

Glucose homeostasis is altered in GHRD individuals. In the *Israeli cohort*, decreased glucose, proportionally increased insulin levels and glucose intolerance are described until puberty, whereas insulinopenia and even insulin resistance is present in adults (Laron et al. 1995). In comparison, the *Ecuadorian cohort* showed higher insulin sensitivity and no cases of diabetes mellitus (Guevara-Aguirre et al. 2015).

Aside from these pathological effects LS possibly facilitates longevity and has protective effects against cancer and diabetes at least in the *Ecuadorian cohort* (Guevara-Aguirre et al. 2011, Laron et al. 2017, Shevah and Laron 2007).

2.5. The growth hormone receptor “null” mouse

To gain clearer understanding of pathophysiological mechanisms of LS and study the role of the GHR in processes such as growth, insulin and glucose metabolism, reproduction and obesity, Zhou et al. (Zhou et al. 1997) established an animal model for LS at the lab of John Kopchick in 1997. Therefore, the major portion of exon 4 and parts of intron 4/5 of the murine *Ghr* gene were deleted by targeted mutation, resulting in no functional GHR (Zhou et al. 1997).

Like in human LS, this defect leads to low IGF1 and elevated GH levels and related dwarfism, obesity, improved insulin sensitivity (as in the *Ecuadorian cohort)*, glucose intolerance, delayed reproductive maturity and, as assumed in human, an extended life span (Basu et al. 2018, Coschigano et al. 2000, List et al. 2011, Liu et al. 2004). While adiposity is normally associated with insulin resistance, metabolic syndrome and diabetes caused by white visceral adipose tissue, *Ghr*-knock out (*Ghr*-KO) mice preferentially accumulate subcutaneous adipose tissue, which is seen as “healthy adiposity”, and have improved insulin sensitivity and glucose tolerance (Berryman et al. 2011, Masternak et al. 2012).

Due to the homogenous genetic background, short generation interval and lifespan, as well as the availability of tissue, this mammalian model accelerated the progress of understanding pathophysiological processes in LS and provided metabolic and functional insight into the somatotropic axis in general (List et al. 2011).

However, this mouse model, like rodent models in general, have several limitations due to physical, but also functional differences to humans like small size, short life expectancy and subtle mechanistical, metabolic and physiological disparities.

2.6. The GHRD pig, a large animal model for human LS

To overcome these limitations of the mouse model Hinrichs et al. generated a *GHR*-knock out (*GHR*-KO) pig as a large animal model for human LS (Hinrichs et al. 2018).

To generate a frameshift mutation in exon 3 of the *GHR* gene, targeted mutation, using the clustered regularly interspaced short palindromic repeats (CRISPR)/CRISPR associated protein 9 (Cas9)-system, was performed in *in vitro* fertilized zygotes of German Landrace pigs. After endoscopic embryo transfer, two female heterozygous founder pigs with an insertion of either one or seven base pairs were born. Breeding of heterozygous filial generation one (F1) offspring from mating with wild-type boars, generated the first homozygous *GHR*-KO pigs.

Like in human LS, *GHR*-KO pigs have distinctly reduced serum IGF1, elevated GH serum levels, transient juvenile hypoglycemia and severe growth retardation. Aside from liver, kidney and heart with reduced and brain with doubled relative weight, the weight of all organs of six-month-old *GHR*-KO compared to control pigs are reduced proportionally to body weight. Increased proportion of body fat and a reduced ratio of muscle to fat tissue clearly show the obese phenotype of *GHR*-KO pigs.

Furthermore, serum levels of leptin and IGFBP2 were increased while levels of IGFBP3 were decreased and serum insulin levels were not changed compared to control pigs (Hinrichs et al. 2018).

As the metabolic phenotype of this large animal model resembles the LS, it is also an appropriate model to evaluate effects of GHRD on hypothalamic energy sensing and negative IGF1 feedback in the hypothalamus and the anterior pituitary gland. Therefore, we investigated total abundance and phosphorylation status of associated hypothalamic and anterior pituitary signaling molecules using sodium dodecyl sulfate polyacrylamide gel electrophoresis (SDS-PAGE) and western immunoblotting techniques.

3. Material and methods

3.1. Material

3.1.1. Tissue

Breeding and tissue sampling have already been performed in a previous project (approved by the responsible animal welfare authority, Regierung von Oberbayern, permission 55.21-54-2532-70-12, according to the German Animal Welfare Act and Directive 2010/63/EU on the protection of animals used for scientific purposes).

GHR-KO animals were generated by breeding of boars and sows with heterozygous mutation of the *GHR* gene.

Dissection and systematically random sampling of fasted *GHR*-KO pigs and control littermates with intact GHR function was performed at the age of six months according to “Tissue Sampling Guides for Porcine Biomedical Models” (Albl et al. 2016).

Humans, mice, and pigs with heterozygous *GHR* mutation show no or exceptionally minor phenotypic features of GHRD with intact GHR signaling (Hinrichs et al. 2018, Riedel et al. 2020, Rosenbloom and Guevara-Aguirre 1998, Rosenbloom et al. 1998, Zhou et al. 1997). Therefore, in accordance to the principle of 3R of Russell and Burch to reduce the number of animals used for research purposes (Russell and Burch 1959), pigs with a heterozygous mutation of the *GHR* gene and wild-type animals were pooled as controls.

Samples were snap-frozen on dry ice and stored at -80 °C until use.

Sample material from the hypothalamus of six *GHR*-KO pigs and six controls was available. Material from anterior pituitary gland of four out of these six pigs per group was used. In both tissues and groups, distribution by sex was equal.

3.1.2. Antibodies

3.1.2.1. Primary antibodies

All primary antibodies were diluted with Tris-buffered saline solution (TBS) with 0.1 % Tween20 (TBS-T) as shown in **Table 1**.

Table 1. Primary antibodies employed for western blot analyses. Company abbreviations: Bio-Rad, Munich, Germany (Bio-Rad); Cell Signaling Technology, Frankfurt, Germany (CST); Merck, Darmstadt, Germany (Merck); Proteintech Europe, Manchester, United Kingdome (PT).

host	antigen	product ID	dilution	company
goat	Human Leptin Receptor	AHP1396	3µg/ml	Bio-Rad
rabbit	Phospho-Leptin receptor (Tyr1077)	#07-1317	1:500	Merck
rabbit	IGF1 Receptor β	#9750	1:1000	CST
rabbit	Insulin Receptor β	#3025	1:1000	CST
rabbit	Phospho-IGF1 Receptor β (Tyr1135/1136) / Phospho-Insulin Receptor β (Tyr1150/1151)	#3024	1:1000	CST
rabbit	IRS-1	#3407	1:1000	CST
rabbit	Phospho-IRS-1 (Ser612)	#3203	1:1000	CST
rabbit	PI3 Kinase p85	#4257	1:1000	CST
rabbit	Phospho-PI3 Kinase p85 (Tyr458) / p55 (Tyr199)	#4228	1:1000	CST
rabbit	AKT (pan)	#4691	1:1000	CST
rabbit	Phospho-AKT (Ser473)	#4060	1:2000	CST
rabbit	GSK3B	#9315	1:1000	CST
rabbit	Phospho-GSK3B (Ser9)	#9322	1:1000	CST
rabbit	AMPKα	#2532	1:1000	CST
rabbit	Phospho-AMPKα (Thr172)	#2535	1:1000	CST
rabbit	mTOR	#2983	1:1000	CST
rabbit	Phospho-mTOR (Ser2448)	#5536	1:1000	CST
rabbit	p70 S6 Kinase	#2708	1:1000	CST
rabbit	Phospho-p70 S6 Kinase (Thr389)	#9205	1:1000	CST
rabbit	eIF4E	#9742	1:1000	CST
rabbit	PPARG	#2435	1:1000	CST
rabbit	GAPDH	#2118	1:5000	CST
rabbit	GHRHR	20715-1-AP	1:500	PT
rabbit	SSTR1	20587-1-AP	1:1000	PT

If the manufacturer did not provide information about reactivity to porcine targets, alignment of the binding regions between validated species and pig was performed to check sequence homology and thus potential reactivity with porcine targets.

3.1.2.2. Secondary antibodies

All secondary antibodies are conjugated with horseradish peroxidase (HRP) for chemiluminescent detection. They were diluted with 2.5 % milk as shown below (**Table 2**).

Table 2. Secondary antibodies employed for western blot analyses.

host	antigen	product ID	dilution	company
donkey	goat IgG	HAF109	1:2500	R&D Systems, Minneapolis, USA
goat	rabbit IgG	#7074	1:2500	Cell Signaling, Frankfurt, Germany

3.1.3. Chemicals

Acetic acid	Roth, Karlsruhe, Germany
Acrylamide, 30 %	SERVA, Heidelberg, Germany
Albumin fraction V, from bovine serum (BSA)	Roth, Karlsruhe, Germany
Aminocaproic acid	AppliChem, Darmstadt, Germany
Ammonium persulfate (APS)	Roth, Karlsruhe, Germany
Aqua bidest Milli-Q®	Merck, Darmstadt, Germany
Bicinchoninic acid solution (BCA)	Sigma, Steinheim, Germany
Bromophenol blue	Sigma, Steinheim, Germany
Copper(II)sulfate, 4 % solution ($CuSO_4$)	Sigma, Steinheim, Germany
Di-sodium hydrogen phosphate (DSP)	Roth, Karlsruhe, Germany
Ethylenediaminetetraacetic acid (EDTA)	VWR, Leuven, Belgium
Glycerol	Roth, Karlsruhe, Germany

Hydrochloric acid, 37 % (HCl)	Roth, Karlsruhe, Germany
2-Mercaptoethanol	Sigma, Steinheim, Germany
Methanol	Merck, Darmstadt, Germany
Phosphatase inhibitor cocktail tablets PhosSTOP	Roche, Mannheim, Germany
Ponceau S	Sigma, Steinheim, Germany
Potassium chloride (KCl)	Merck, Darmstadt, Germany
Potassium dihydrogen phosphate (KDP)	Merck, Darmstadt, Germany
Powdered milk	Roth, Karlsruhe, Germany
Protease inhibitor cocktail tablets cOmplete	Roche, Mannheim, Germany
Sodium dodecyl sulfate (SDS)	SERVA, Heidelberg, Germany
Sodium chloride (NaCl)	Merck, Darmstadt, Germany
Tween® 20	Sigma, Steinheim, Germany
Tetramethylethylenediamine (TEMED)	Roth, Karlsruhe, Germany
Tris(hydroxymethyl)aminomethan (Tris)	Roth, Karlsruhe, Germany

3.1.4. Buffers, media, solutions

PBS:	137 mM NaCl, 2.7 mM KCl, 8 mM DSP, 1.5 mM KDP
CuSO4-BCA-solution:	0.08 % CuSO4 in BCA
Lower sol:	1.5 M Tris/HCl, pH 8.8 + SDS
Upper sol:	0.5 M Tris/HCl, pH 6.8
Lower gel 10 % (1 gel):	3.125 ml aqua bidest, 1.875 ml lower sol, 2.5 ml acrylamide, 75 µl APS, 5 µl TEMED
Upper gel (1 gel):	3.05 ml aqua bidest, 1.3 ml upper sol, 0.65 ml acrylamide, 50 µl APS, 5 µl TEMED

SDS-running buffer:	25 mM TRIS, 0.2 mM Glycine, 0.1 % SDS
Cathode buffer:	25 mM TRIS, 40 mM aminocaproic acid, 0.01 % SDS, 20 % methanol
Membrane buffer:	25 mM TRIS, 20 % Methanol
Anode buffer I:	0.3 M TRIS, 20 % Methanol
Paunceau-S-solution:	3 % acetic acid, 0.2 % Ponceau-S
TBS:	137 mM NaCl, 25 mM TRIS/HCl, pH 7.4
TBS-T (0.1 %):	TBS, 0.1 % Tween® 20
2.5/5 % milk:	2.5/5 % powdered milk in TBS-T
2.5/5 % BSA:	2.5/5 % BSA in TBS-T
Elution buffer:	2.5 % SDS, 62.5 mM Tris/HCl, pH 6.7, 90 mM beta-mercaptoethanol
5x Laemmli buffer:	0,3125 M Tris/HCl, pH 6.8, 5.43 M/50 % glycerol, 10 % SDS, 1 % bromophenol blue; 1 tablet PhosSTOP (Roche) and 1 tablet cOmplete (Roche) per 20 ml 1x Laemmli buffer

3.1.5. Consumables

96-well-F dish	Corning, Corning, USA
Blotting paper, 703 (0.38 mm)	VWR, Radnor, USA
Blotting paper extra thick (2.45 mm)	Bio-Rad, Hercules, USA
Gel blotting paper (GB002) (whatman paper)	Schleicher & Schüll, Dassel, Germany
Gelloader pipette tips (0.1-200 µl)	Sarstedt, Nümbrecht, Germany
Immobilon-P Transfer Membrane	Merck, Darmstadt, Germany
PageRuler prestained protein ladder (10-180 kD)	Thermo fisher, Waltham, USA

Parafilm M	Bemis, Neenah, USA
Pipette tips (0.1-10 µl, 250 µl, 1000 µl)	Eppendorf, Hamburg, Germany
Safe-Lock tubes (1.5 ml, 2 ml)	Eppendorf, Hamburg, Germany
SuperSignal™ West Chemiluminescent Substrate	Thermo fisher, Waltham, USA
TissueTUBE Extra Thick TT05/TT1	Covaris Inc., Massachusetts, USA
Tube (10 ml, 50 ml)	Sarstedt, Nümbrecht, Germany

3.1.6. Devices

In addition to basic laboratory equipment, the following devices were used:

Centrifuge 5417R	Eppendorf, Hamburg, Germany
CO_2-Incubator	Memmert, Schwabach, Germany
CP02 cryoPREP Automated Dry Pulverizer (110V)	Covaris Inc., Massachusetts, USA
ECL ChemoStar chemiluminescence imager	Intas, Göttingen, Germany
Hybridization oven	Bachofer, Reutlingen, Germany
Mini-PROTEAN® Tetra System	Bio-Rad, Hercules, USA
PowerPac™ Basic Power Supply	Bio-Rad, Hercules, USA
SONOPULS Ultrasonic homogeniser	BANDELIN, Berlin, Germany
Sunrise™absorbance microplate reader	Tecan, Männedorf, Switzerland
Thermomixer 5436	Eppendorf, Hamburg, Germany
Trans-Blot® Turbo™ Transfer System	Bio-Rad, Hercules, USA

3.1.7. Software

Magellan™	Tecan, Männedorf, Switzerland
ImageJ 1.53e	Wayne Rasband, NIH, USA

SPSS Modeler V17.1	IBM, New York, USA
Prism 5.04 for Windows	GraphPad Software, San Diego, USA

3.2. Methods

To guarantee enough protein for targeted and especially for non-targeted proteome analysis (mass spectrometry) and because of limitations due to the low sample amount, the protein yields per milligram tissue of hypothalamus and anterior pituitary gland were tested with surplus material of control animals. Sample preprocessing and concentration measurement, as well as further processing and detection of both methods mentioned above were performed to practice and ensure precise performance.

Because of the tremendous amount of results in non-targeted proteome analysis using mass spectrometry of 4712 identified proteins and 18 significant different abundant proteins after false discovery rate (FDR) correction (FDR < 0.05; log2foldchange > 0.6) in hypothalamus and 4660 identified proteins and 592 significant different abundant proteins after FDR correction (FDR < 0.05; log2foldchange > 0.6) in anterior pituitary gland and the limited extent of this thesis, neither the method nor the results of non-targeted proteomics are topics of this thesis.

If not described in another manner, samples of each animal and organ were not pooled but individually processed.

3.2.1. Sample preprocessing

Because of the extensive analysis planned and the limited amount of sample material, homogenous splitting was an important tool to generate comparable material for targeted and non-targeted proteome analysis.

Therefore, reproducible pulverization of the available frozen material was performed using tissueTUBEs (TissueTUBE Extra Thick TT05/TT1, Covaris Inc., USA) and an

automated dry pulverizer (CP02 cryoPREP (110V), Covaris Inc., USA) by one impact at impact level four.

First, 10 mg per sample of hypothalamus and 3 mg per sample of anterior pituitary gland were used for mass spectrometric proteome analysis. The remaining amount of the frozen and pulverized tissue was used for targeted proteome analysis in this thesis.

3.2.2. Protein extraction

To reach volumes that enable proper handling and still have adequate concentration, the rest of the frozen material, 10.3-17.1 mg of hypothalamus and 3.0-17.5 mg of anterior pituitary gland, was dispensed in 100 µl of Laemmli buffer in safe-lock tubes. Laemmli buffer combines effects of TRIS, glycine and SDS. Especially SDS plays a major role in protein cleavage (Laemmli 1970).

Subsequently, homogenization with an ultrasonicator (SONOPULS Ultrasonic homogenizer, BANDELIN, Germany) was performed with a mean energy of approximately 21700 MJ to dissolve the tissue properly.

Protein samples were denatured for five minutes at 95 °C. Basis for this process are SDS-anions, from Laemmli buffer, forming micelle-like clusters along the polypeptide chain, giving them a negative charge and destroying the quaternary, tertiary and secondary protein structure, resulting in an elongated amino acid chain (Guo et al. 1990, Winogradoff et al. 2020).

After storage on ice for five minutes and centrifugation for five minutes at 4 °C and 20200 xg, the solved protein solution was transferred to new safe-lock tubes.

3.2.3. Protein concentration measurement

To estimate protein concentration, a bicinchoninic acid (BCA) assay, first described by Smith et al.(Smith et al. 1985), was performed. In this protein assay, Cu^{2+} ions are

reduced by amide groups of peptide bonds to Cu^{+}, which form, in an alkaline environment, $Cu^{+}(BCA)_2$ complexes with a typical purple color (Walker 1994).

A serial dilution of bovine serum albumin (BSA) was prepared in PBS to create protein standards that range from 8 mg/ml - 0.0125 mg/ml.

10 µl of all samples and the BSA standards were diluted by factor five with PBS, vortexed and stored on ice. After adding 200 µl of $CuSO_4$-BCA-solution to the diluted standards and samples, duplicates of 110 µl each were pipetted into a 96-well-F dish and incubated for 30 minutes at 37 °C in a CO_2-Incubator.

Afterwards, light absorption was measured at 560 nm with an ELISA-Reader (Sunrise™absorbance microplate reader, Tecan, Switzerland).

Data processing was performed by Magellan™ (Tecan, Switzerland) and the absolute concentrations were calculated using Microsoft Excel.

3.2.4. Electrophoretic protein separation

To separate proteins by their molecular weight, SDS-PAGE was performed using Mini-PROTEAN® Tetra System (Bio-Rad, USA). In this process the elongated proteins run through a polymer gel of acrylamide, the smaller the faster and vice versa, driven by their negative charge and the distributed voltage (Weber and Osborn 1969).

To accumulate proteins from the gel cavities, the first few millimeters are characterized by a wide polymer net (upper gel), followed by a polymer net with smaller pores (lower gel) to obtain good separation by molecular weight.

When pouring the lower gel between the vertical placed double glass plate system bidestilled water was placed on top to get a straight upper edge. After a polymerization time of at least 60 minutes at room temperature, the water on top was removed and the upper gel was poured onto the lower gel. Immediately gel combs, 15-well comb for hypothalamus samples and 10-well combs for anterior pituitary samples, were put in. After at least 30 minutes of polymerization at room temperature the gel combs were removed.

15 µg protein per sample dissolved with Laemmli buffer were used. To elongate proteins additionally to SDS effect, diluted samples were denaturized for five minutes at 95 °C with 1 µl 2-mercaptoethanol per sample to break disulfide bonds. Afterwards, they were stored on ice for two minutes and condensate was short centrifuged.

After preparing the rest of the system (Mini-PROTEAN® Tetra System, Bio-Rad, USA) and filling it with 1xSDS-running buffer, gel combs were pulled. This leaves rows of gel pockets, which were first filled with 5 µl of prestained protein ladder and then with either 15 µg protein of each hypothalamus sample or 15 µg protein of each anterior pituitary gland sample. For electrophoresis, the power supply (PowerPac™ Basic, Bio-Rad, USA) was used at 80 V until the marker and the samples reached the lower gel, then voltage was switched to 140 V. After the marker band of 34 kD (lightest protein of interest: glyceraldehyde 3-phosphate dehydrogenase (GAPDH) with 36 kD) reached 1 cm before the end of the gel, electrophoresis was stopped.

3.2.5. Semi-dry blotting

To blot the negative charged proteins on to an Immobilon®-P transfer membrane, current flow of a Trans-Blot® Turbo™ blotting system (Bio-Rad, USA) was used. This type of electric transfer from SDS-PAGE was first described by Towbin et al. (Towbin et al. 1979).

For preparation the transfer membranes were labeled, activated for ten minutes in methanol and afterwards incubated for at least 20 minutes in the membrane buffer. Whatman papers were soaked in anode-, membrane- and cathode buffer. All materials were cut into the same size as the SDS-PAGE gel.

The gel was separated from the glass plates and transferred to a stack as illustrated below (**Table 3**).

Table 3. Order of the transfer stack.

Material	**Additional preparation**
Anode of blotting cassette	
Whatman paper 2.45 mm	soaked in anode buffer
Whatman paper 0.38 mm	soaked in membrane buffer
Immobilon®-P Transfer Membrane	activation in methanol, soaked in membrane buffer
SDS-PAGE gel	
Whatman paper 2.45 mm	soaked in cathode buffer
Cathode of blotting cassette	

To guarantee proper and homogenous transfer, the gel was placed bubble free and cassette was closed tightly.

Proteins were transferred at 25 V for 75 minutes resulting in 0.1 A per cassette. After blotting, transfer control was performed using Ponceau-S solution. To preserve the molecular weight marker from getting lost, bands were marked with a ballpoint pen. Furthermore, membranes were cut to analyze targets with higher molecular weight on the upper part and targets with lower molecular weight on the lower part. This allowed the examination of more targets of interest despite of limited sample material.

3.2.6. Immunoblotting and detection

Membranes were washed (three times for ten minutes at room temperature in TBS-T) and blocked in 5 % milk for one hour at room temperature (RT). After washing as described previously, membranes were incubated overnight (hybridization oven, Bachofer, Germany) at 4 °C with diluted primary antibodies. Afterwards, membranes were incubated with appropriate secondary horseradish peroxidase (HRP) conjugated

antibodies for one hour (hybridization oven, Bachofer, Germany) at RT. Before and after the incubation with secondary antibodies, membranes were washed.

All antibodies and their dilutions are provided in chapter 3.1.2.

Immunoreactive bands were visualized via antibody bond HRP metabolizing its substrate (SuperSignal™ West Chemiluminescent Substrate, Thermo fisher, USA) and a chemiluminescence imager (ECL ChemoStar, Intas, Germany).

3.2.7. Stripping of membranes

To analyze the phosphorylation status as well as the expression of the total protein and the reference proteins on the same blot, stripping was performed. Therefore, membranes were incubated (hybridization oven, Bachofer, Germany) in elution buffer for 40 minutes at 70 °C and washed twice for ten minutes with aqua bidest at RT. Afterwards, immunoblotting and detection (3.2.6) was repeated.

Because of the sensitivity of phosphorylated protein domains to stripping, detection of these targets is not possible anymore. Thus, stripped membranes were just used with antibodies for total targets.

3.2.8. Quantitative imaging, statistical analysis and illustration

After checking the quality and accuracy of the bands on chemiluminescence images, intensities were quantified using ImageJ (version 1.53e, Wayne Rasband, USA).

To analyze phosphorylation status, the abundance of phosphorylated proteins in relation to total counterparts was determined. To evaluate differences in total targets, intensities were normalized with intensities of the loading control GAPDH. To analyze differences between groups of genotype, groups of sex, and the interaction of both groups in the hypothalamus, two-way analysis of variance (ANOVA) was performed using SPSS (version V17.1, IBM, USA), after verification of Gaussian distribution using the Kolmogorov–Smirnov test. Because of small sample size in anterior pituitary gland,

data of groups of sex or genotype were compared by non-parametric Mann–Whitney U test using SPSS (version V17.1, IBM, USA).

Group differences were considered to be statistically significant if $p < 0.05$.

To illustrate results, boxplots and scatterplots were generated using Prism (version 5.04, GraphPad Software, USA).

4. Results

To investigate the effects of LS on central regulatory mechanisms of endocrine feedback-loops and metabolism, we investigated total protein abundance and phosphorylation of downstream signaling cascades of IGF1R and LEPR. A general overview of the current knowledge is given in chapter 2 (review of the literature) and a schematic summery is provided in **Figure 3**.

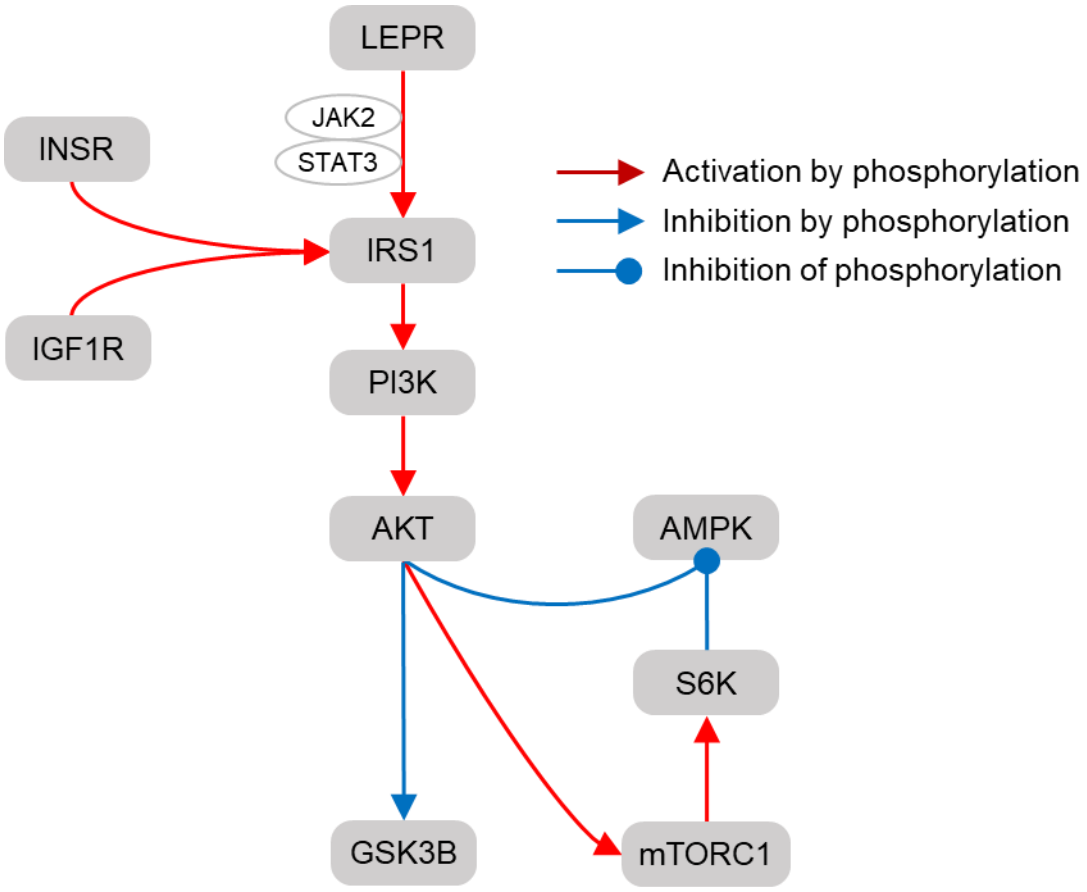

Figure 3. Schematic summary of signaling related with IGF1R and LEPR. Arrows show reported knowledge about activation and inhibition in these cascades. For multiple references see chapter 2.

4.1. Increased phosphorylation of IRS1 pathway but not mTOR in *GHR*-KO hypothalami

The abundance of total target proteins (p = 0.21-0.95) and GAPDH (p = 0.61) in samples of hypothalamus was not significantly different between *GHR*-KO and control pigs. Only S6K showed a trend (p = 0.052) towards increased abundance in *GHR*-KO compared with the controls (**Figure 4**).

Antibodies against peroxisome proliferator-activated receptor gamma (PPARG) and total LEPR had low affinity to these targets and thus supplied no analyzable results.

GHR-KO samples of hypothalamus showed a significant increase in phosphorylation of IRS1 (p = 0.006) compared to controls. Further investigation of signal transducers downstream of IRS1 revealed significantly increased phosphorylation of AKT (p = 0.002) and glycogen synthase kinase 3 beta (GSK3B) (p = 0.046) in *GHR*-KO pigs, but no significant (p = 0.699) changes in PI3K (**Figure 5A**).

Furthermore, phosphorylation of AMPK was significantly (p = 0.019) increased in *GHR*-KO pigs. The phosphorylation status of mTOR (p = 0.988) and S6K (p = 0.382) were not significantly different (**Figure 5B**). There were no targets with a decrease in phosphorylation status in *GHR*-KO pigs compared to controls.

The antibody against phosphorylated IGF1R/INSR (pIGF1R/pINSR) had low affinity to the targets and thus supplied no analyzable results.

In contrast to phosphorylated leptin receptor protein (pLEPR), the affinity of the antibody used for the detection of LEPR abundance was too low for a sufficient determination. Therefore, to get an impression of LEPR phosphorylation status between groups, results of pLEPR were normalize with the loading control GAPDH. The abundance of pLEPR in *GHR*-KO pigs was significantly increased, as the determined effect for genotype had a p-value of 0.006 (**Figure 6**).

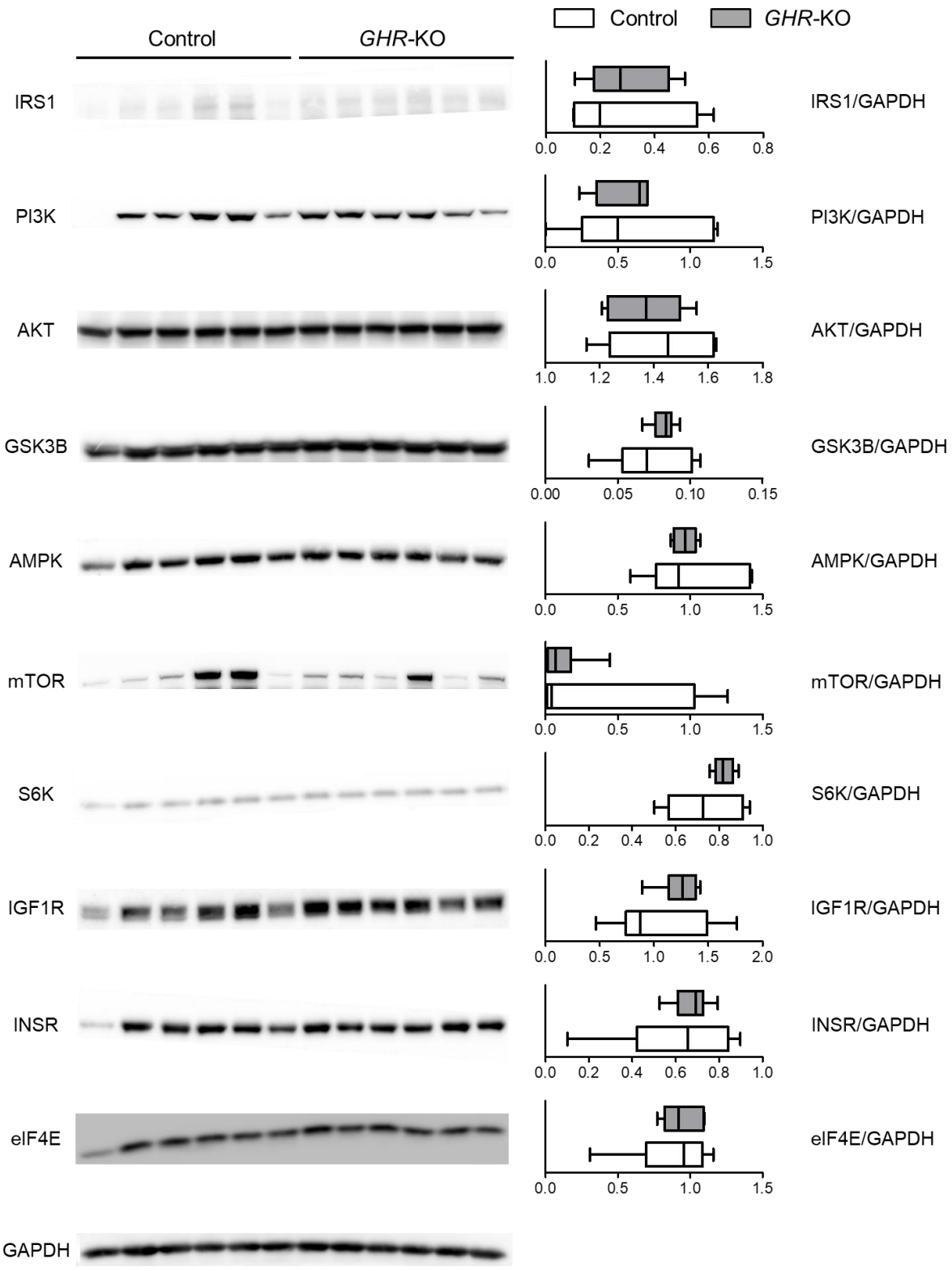

Figure 4. Western blot analysis of total proteins related to the INSR/IGF1R and LEPR signaling pathways in samples of hypothalamus of six-month-old fasted GHR-KO (n = 6) and control pigs (n = 6). Box plots show medians, 25th and 75th percentiles (box), and maximums/minimums (whiskers). No significant differences between groups were observed; main effect of genotype groups evaluated using two-way ANOVA.

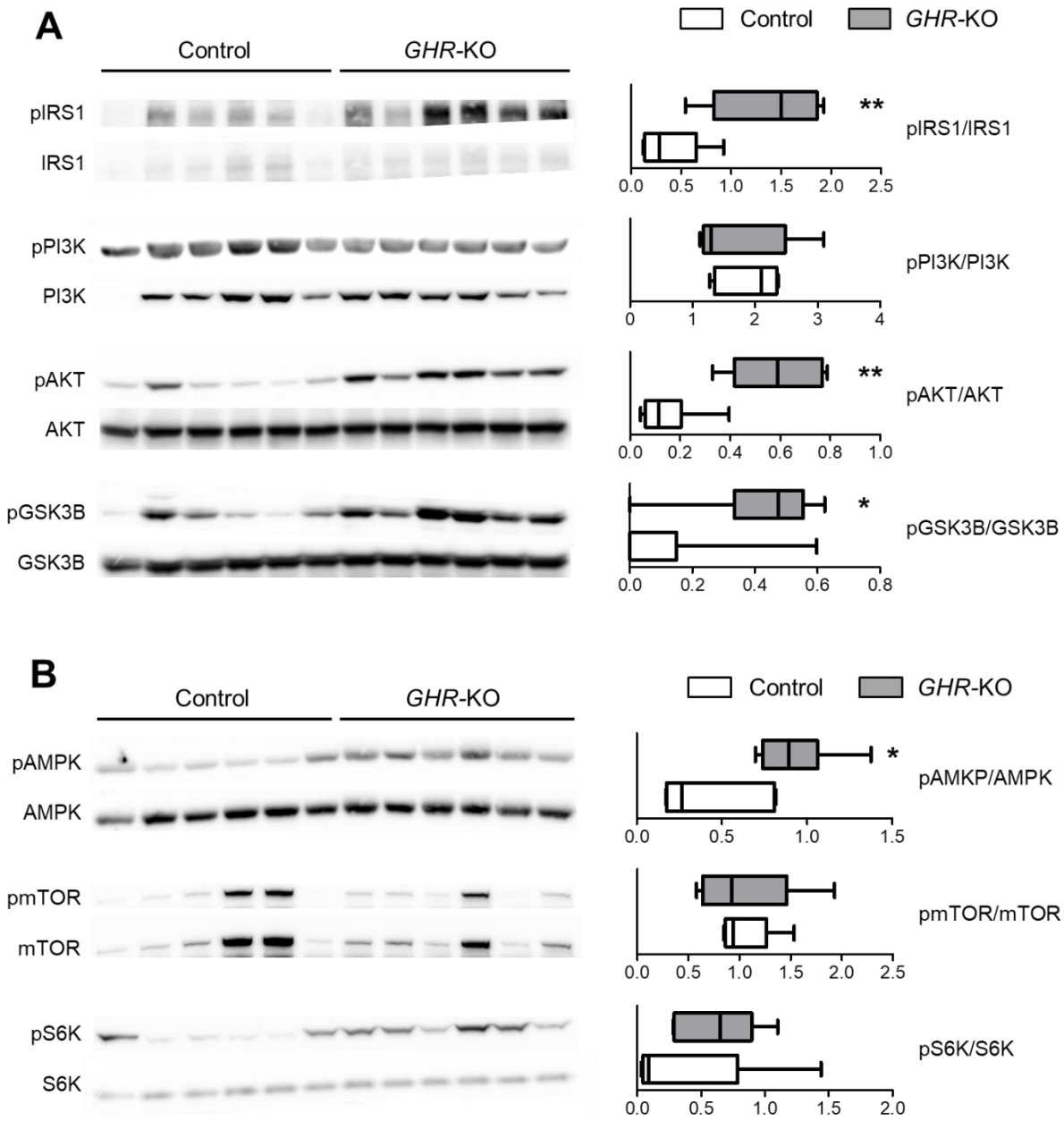

*Figure 5. Western blot analysis of phosphorylation status of IRS1 and the downstream signaling cascade (A) and LEPR related signaling proteins (B) in samples of hypothalamus of six-month-old fasted GHR-KO (n = 6) and control pigs (n = 6). Box plots show medians, 25th and 75th percentiles (box), and maximums/minimums (whiskers). **p < 0.01; *p < 0.05; main effect of genotype groups evaluated using two-way ANOVA.*

A summary of the results concerning phosphorylation status in hypothalamus of *GHR*-KO pigs compared to controls is provided in **Figure 7**.

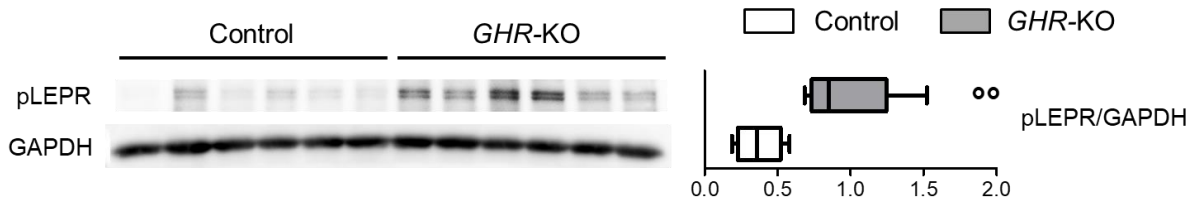

Figure 6. Western blot analysis of phosphorylated pLEPR in samples of hypothalamus of six-month-old fasted GHR-KO (n = 6) and control pigs (n = 6). Box plots show medians, 25th and 75th percentiles (box), and maximums/minimums (whiskers). (°°)p = 0.006; main effect of genotype groups evaluated using two-way ANOVA.

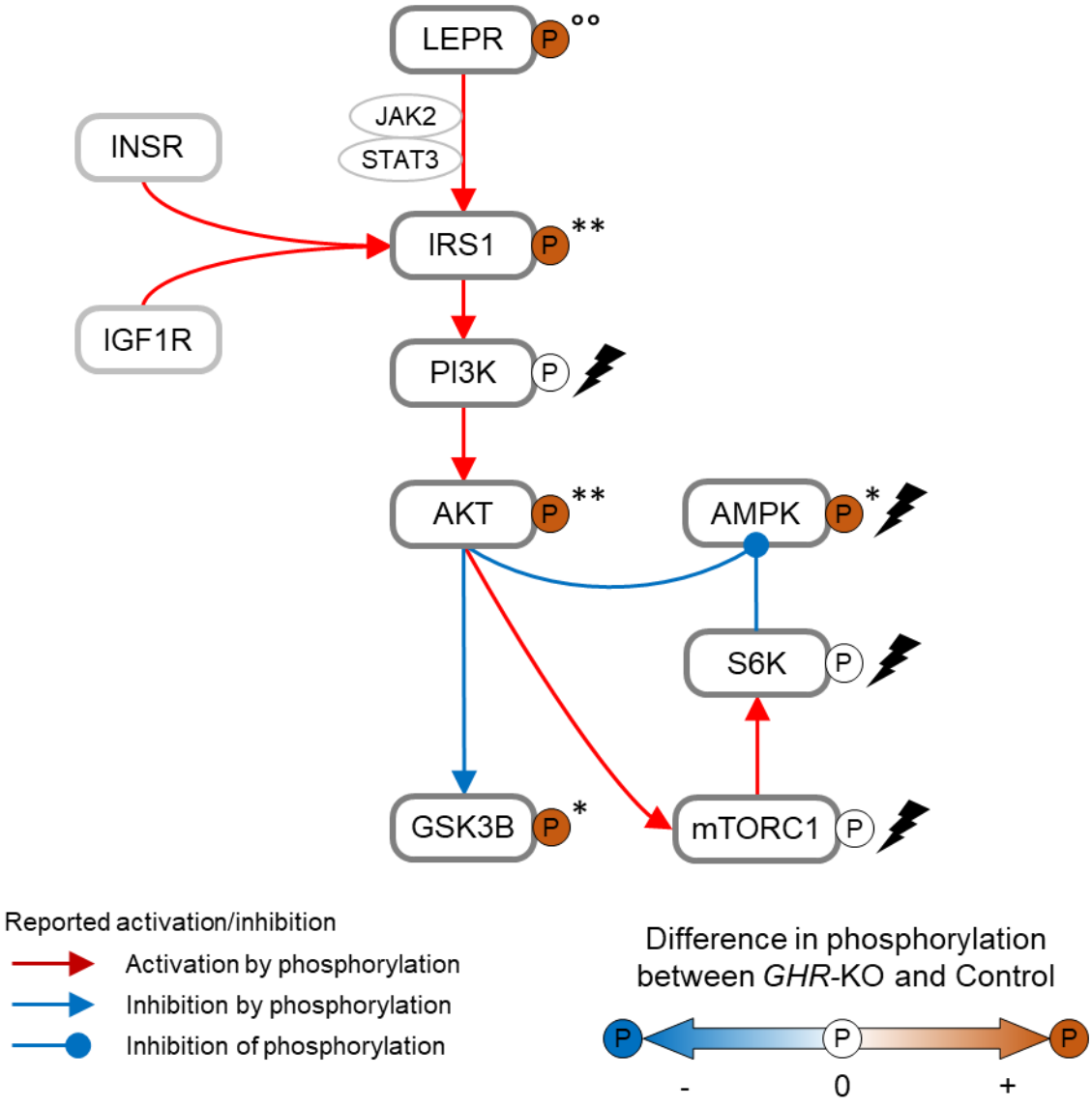

*Figure 7. Schematic summary of changes in phosphorylation status in IGF1R/INSR and LEPR signaling in samples of hypothalamus of six-month-old fasted GHR-KO compared to control pigs. Lightning flash marks unexpected findings. pLEPR/GAPDH: (°°)p = 0,006; phosphor targets/total targets: **p < 0.01; *p < 0.05; main effect of genotype groups evaluated using two-way ANOVA.*

4.2. Hypothalamic sex differences in total protein abundances but not phosphorylation status

Compared with no differences perceived in the abundance of total target proteins between groups of genotype, significant differences between groups of sex in hypothalamus could be determined. The significantly different proteins IRS1 ($p = 0.039$), AKT ($p = 0.003$), GSK3B ($p = 0.014$), AMPK ($p = 0.049$) and S6K ($p = 0.003$) were expressed higher in female compared to male pigs (**Figure 8**).

Statistics of groups of sex in terms of phosphorylation status revealed no significant differences (**Figure 9**).

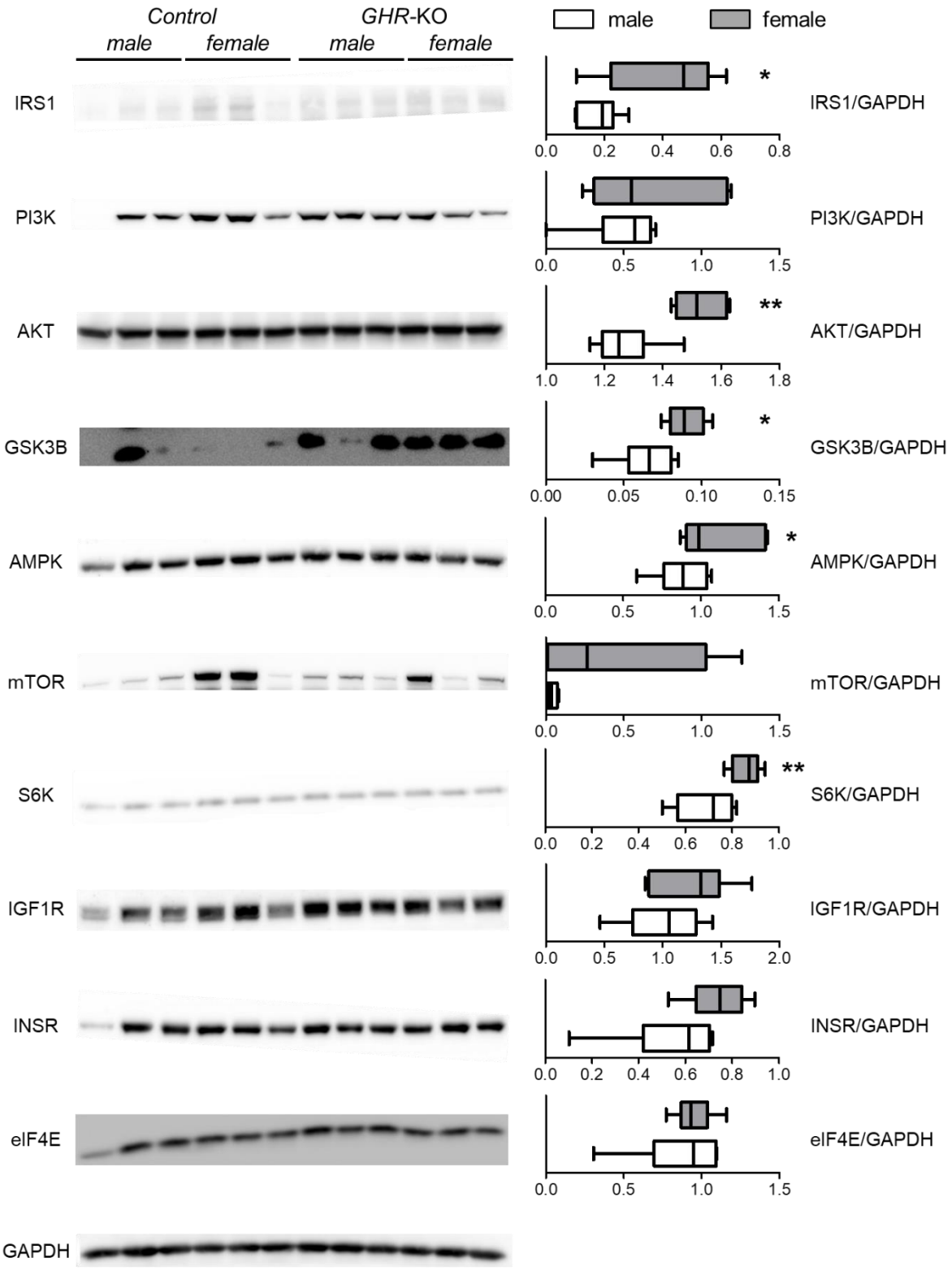

*Figure 8. Western blot analysis of total proteins related to the INSR/IGF1R and LEPR signaling pathways in samples of hypothalamus of six-month-old fasted female (n = 6) and mal pigs (n = 6). Box plots show medians, 25th and 75th percentiles (box), and maximums/minimums (whiskers). **p < 0.01; *p < 0.05; main effect of groups of sex evaluated using two-way ANOVA.*

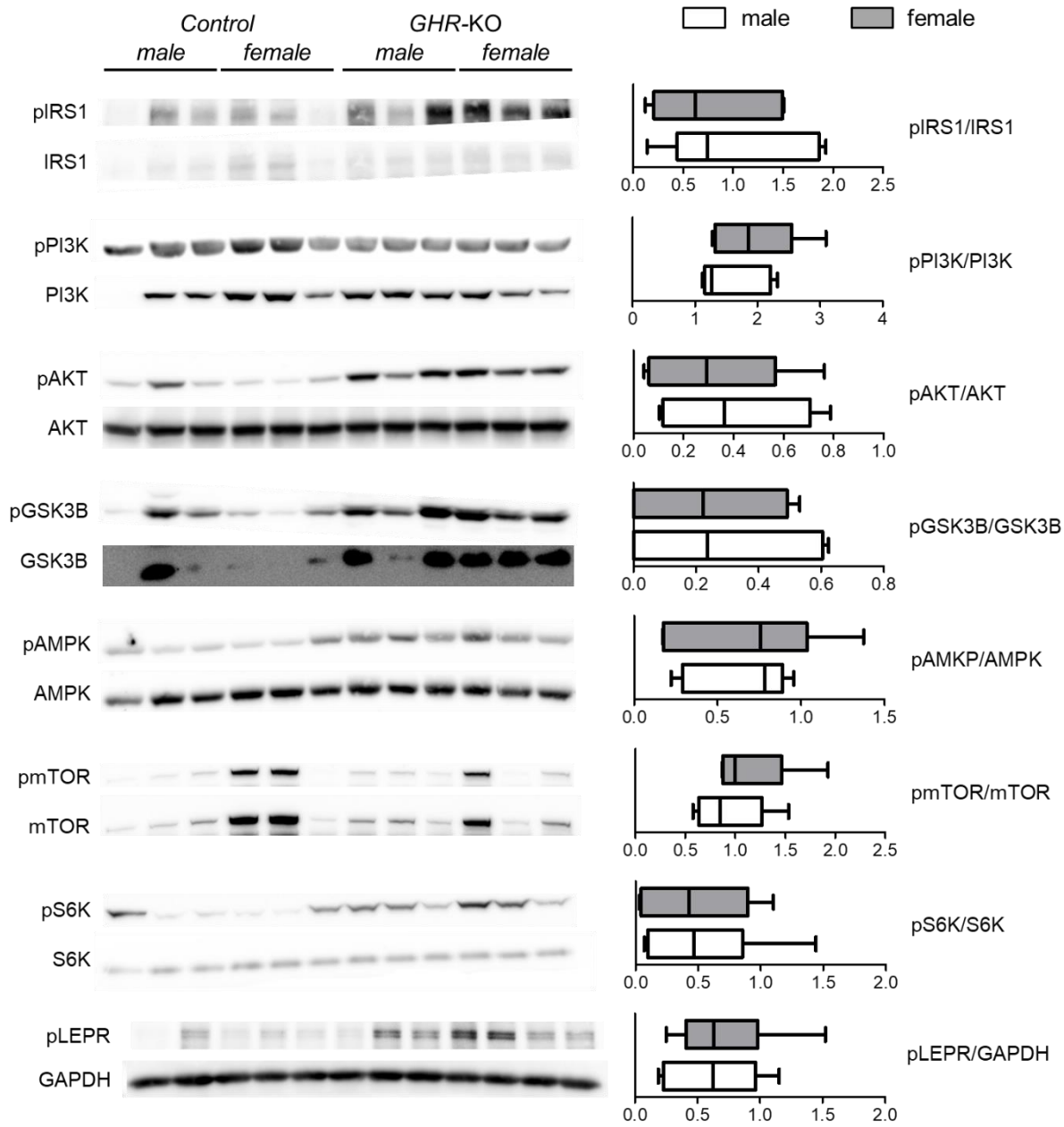

Figure 9. Western blot analysis of phosphorylation status of IRS1, LEPR and related signaling proteins in samples of hypothalamus of six-month-old fasted female (n = 6) and male pigs (n = 6). Box plots show medians, 25th and 75th percentiles (box), and maximums/minimums (whiskers). No significant differences between groups were observed; main effect of groups of sex evaluated using two-way ANOVA.

4.3. Two-way ANOVA reveals differences in variance in *GHR*-KO hypothalami

Two-way ANOVA revealed few significant differences in hypothalami between the four groups of sex and genotype.

Total protein abundance between groups was significantly different in AMPK ($p = 0.017$) and S6K ($p = 0.028$) with a lower variance and clustering of groups of sex in *GHR*-KO, visualized in **Figure 10A**.

Analysis of phosphorylation status of mTOR between the four groups revealed significant differences ($p = 0.022$) but with a higher variance in *GHR*-KO pigs (**Figure 10B**).

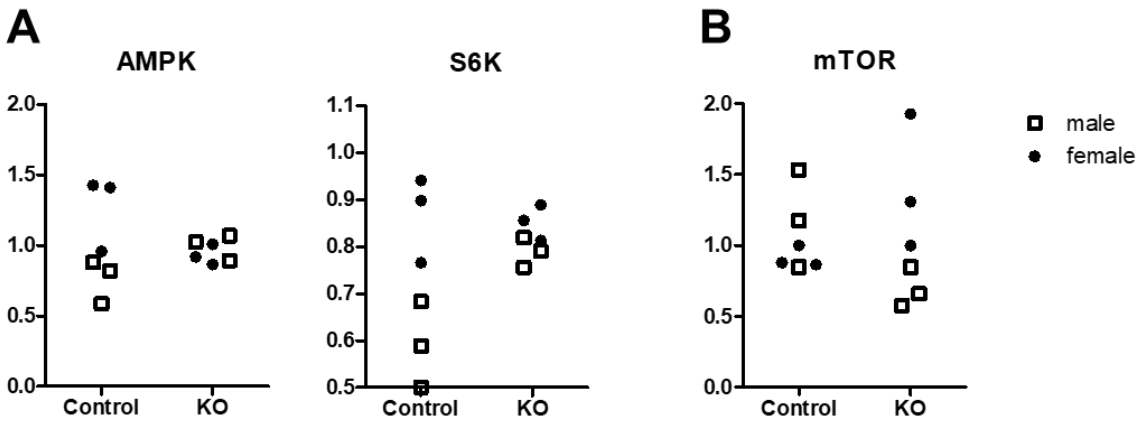

*Figure 10. Scatterplots of in two-way ANOVA significantly different total protein abundance of AMPK and S6K (A) and phosphorylation status of mTOR (B) in samples of hypothalamus of six-month-old fasted male (n = 3) and female (n = 3) GHR-KO and male (n = 3) and female (n = 3) control pigs; interaction effect of genotype*sex groups evaluated using two-way ANOVA.*

4.4. Increased pIRS1 in anterior pituitary glands of *GHR*-KO pigs

As in hypothalamus, the total amount of all total targets in anterior pituitary gland samples was not significantly different between groups of genotype (IRS1 $p = 0.1143$, mTOR $p = 0.3429$, IGF1R $p = 0.20$, INSR $p = 0.3429$, SSTR $p = 0.1143$, GAPDH $p = 0.14$-0.52) **(Figure 11)**.

The antibody against GHRH receptor (GHRHR) had low affinity to the targets and thus supplied no analyzable results.

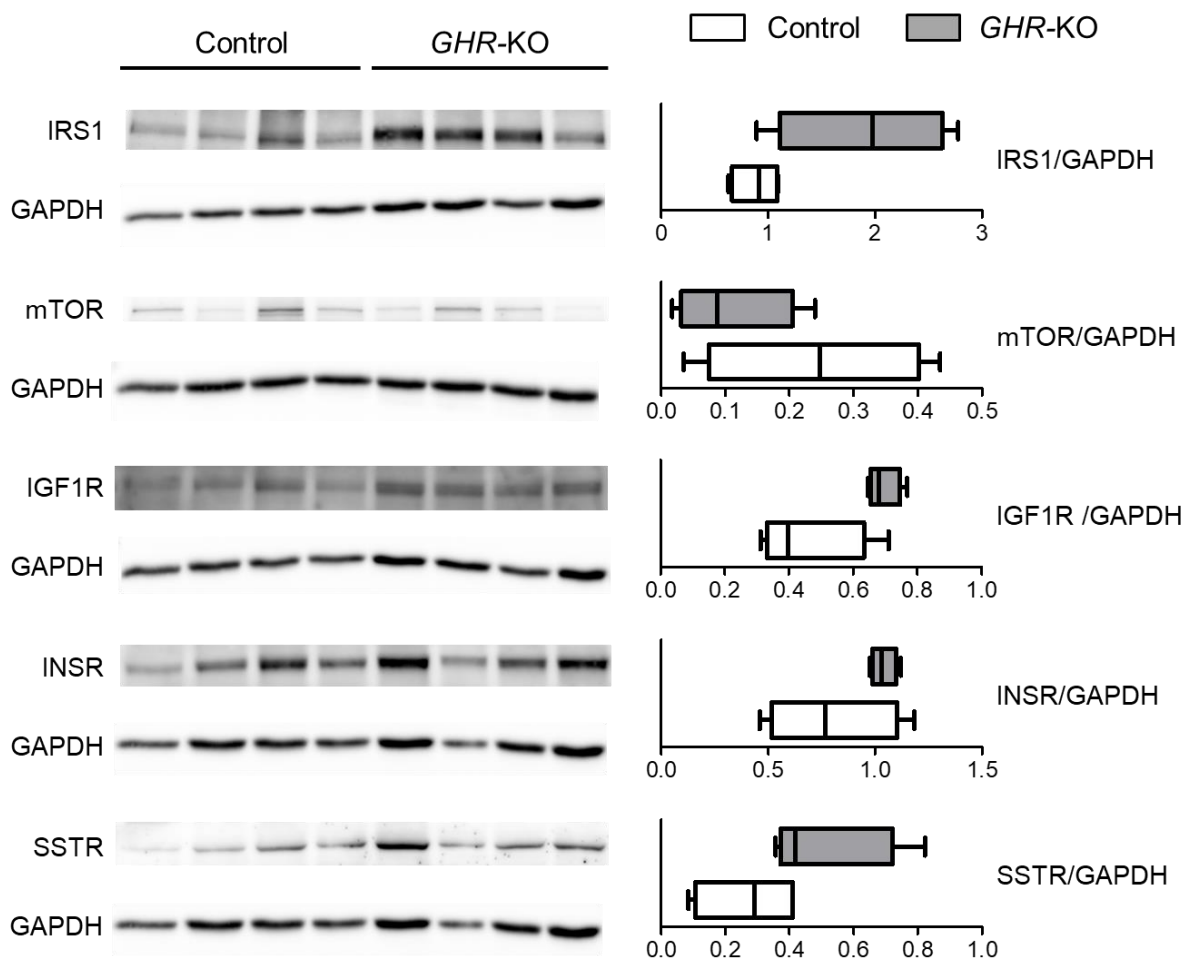

Figure 11. Western blot analysis of total targets in samples of anterior pituitary gland of six-month-old fasted GHR-KO (n = 4) and control pigs (n = 4). Box plots show medians, 25th and 75th percentiles (box), and maximums/minimums (whiskers). No significant differences between groups of genotype; evaluated using the Mann-Whitney U test.

Phosphorylation status of IRS1 was significantly ($p = 0.029$) increased and a trend ($p = 0.0571$) towards increased mTOR could be determined in anterior pituitary of *GHR*-KO pigs compared to controls (**Figure 12**).

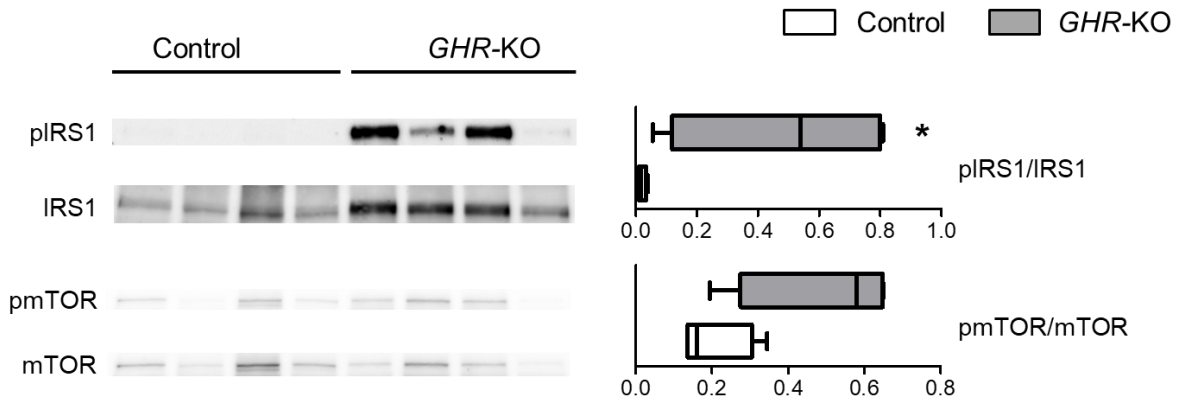

*Figure 12. Western blot analysis of phosphorylation status of IRS1 and mTOR in anterior pituitary gland samples of six-month-old fasted GHR-KO (n = 4) and control pigs (n = 4). Box plots show medians, 25th and 75th percentiles (box), and maximums/minimums (whiskers). *p < 0.05; evaluated using the Mann-Whitney U test.*

4.5. No sex differences in investigated targets in pituitary tissue

Statistics revealed no significant sex differences, neither in phosphorylation status (**Figure 13A**) nor in total protein abundance (**Figure 13B**).

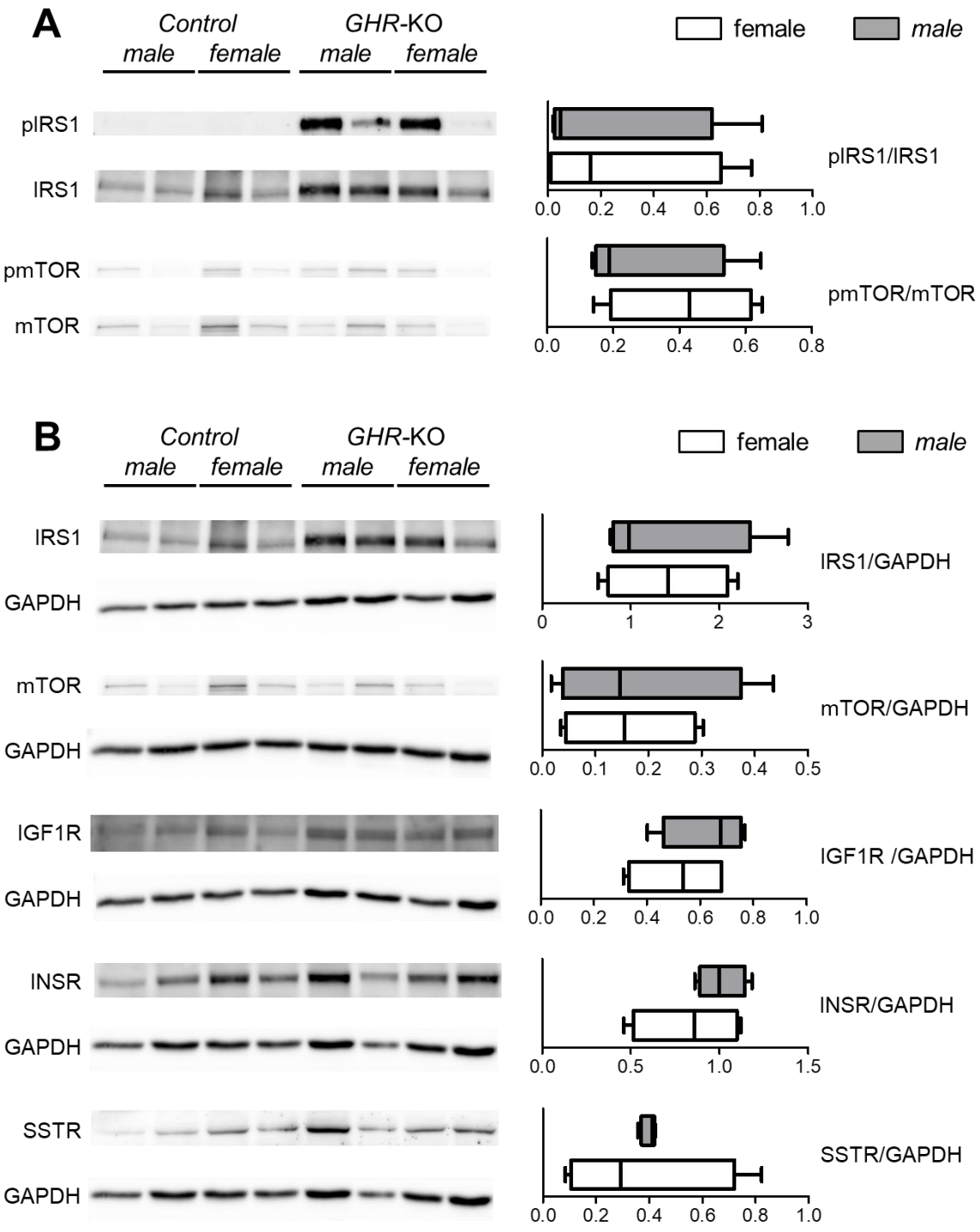

Figure 13. Western blot analysis of phosphorylation status (A) and total protein abundance (B) of target proteins in samples anterior pituitary gland of six-month-old fasted female (n = 4) and male pigs (n = 4). Box plots show medians, 25th and 75th percentiles (box), and maximums/minimums (whiskers). No significant differences between groups of sex; evaluated using the Mann-Whitney U test.

5. Discussion

Classical immunoblotting methods, as performed in this thesis, have the advantage of high sensitivity, even at amounts of few femtomoles, but are limited due to availability and quality of primary antibodies (Reinders and Sickmann 2005). Even though we used only primary antibodies that are validated for pig by the distributing company or having high sequence homology between binding regions of validated species and pig, some had low or even no reactivity to the respective target. This reveals a common problem working with pig tissue in terms of rodent focused biomedical research, where antibodies are mostly validated for human and rodents and annotation of the porcine genome, needed for proper alignment, is less sophisticated than in human or mice (Beiki et al. 2019, Summers et al. 2020).

To reveal the activity of intracellular signaling cascades, the investigation of reversible protein phosphorylation, one of the most important post translational modifications, is essential in biomedical research (de Graauw et al. 2006, Mukherji 2005, Reinders and Sickmann 2005). In this study, differences in phosphorylation status but not in total protein abundance between *GHR*-KO and control pigs show that phospho-studies of IGF1 and leptin related signaling in hypothalamus and the anterior pituitary gland are important for the analysis of these cascades and give an impression of their activity.

As opposed to this, sex-related differences in hypothalami are not represented as differences in phosphorylation (=activity), but in total protein abundance. This might show that activity is comparable between groups of sex despite different total protein abundance. Two-way ANOVA revealed that *GHR*-KO pigs seem to have significantly less sex-related differences in total protein abundance of AMPK and S6K compared to controls. In contrast, statistics revealed more sex-related differences in mTOR activity of *GHR*-KO compared to control pigs, but without differences between groups of sex or groups of genotype. As we are interested in differences in the activity of cascades between *GHR*-KO and control pigs and we discovered no differences in phosphorylation (=activity) between groups of sex, only genotype differences are discussed further on.

Box plots of non-significantly different targets in anterior pituitary gland (Figures 9 and 10) suggest trends of differences between *GHR*-KO and control pigs in total IRS1, IGF1R and SST as well as phosphorylation of mTOR. Because of the low sample size per group and the suggested trends, these results showing no statistical differences must be seen critical and should be re-evaluated with a bigger sample size.

A principle problem with analysis of inhomogeneous tissues compared to homogenous cell lines is the composition of different cell types. Especially in hypothalamus, two cell types and their differences in signaling play a role. In POMC neurons, leptin activates PI3K signaling and inhibits it in AGRP neurons. In contrast, insulin increases PI3K activity in both cell types (Xu et al. 2005). This can lead to difficulties in interpretation and validity of results from inhomogeneous tissues.

5.1. Differences in LEPR, INSR and IGF1R signaling

The determined upregulation of phosphorylated LEPR and downstream signaling molecules in hypothalami of six-month-old *GHR*-KO pigs derive from significantly increased fasting serum leptin concentrations, described in *GHR*-KO pigs with same pedigree and age (Hinrichs et al. 2018). These elevated leptin levels from adipose tissue can be explained in two ways: On the one hand GH dependent suppression of leptin production is lost due to GHRD (Considine et al. 1996, Maffei et al. 1995, Rosenbaum et al. 1996). And/or higher body fat percentage, as it is described in *GHR*-KO compared to control pigs (21.5 ± 0.7 % vs. 11.4 ± 0.5 % (Hinrichs et al. 2018)), increases leptin levels.

The evaluation of downstream cascades of LEPR, INSR and eventually IGF1R via IRS1 revealed a significant upregulation in phosphorylation of IRS1, AKT and GSK3B in hypothalami of *GHR*-KO pigs compared to controls. Contrary to IRS1 and AKT, hypothalamic PI3K, a signal transducer between IRS1 and AKT, shows no significant differences in phosphorylation at its subunit p55. The relevant subunits for this pathway (catalytic subunit p110 and regulatory subunit p85) could not be determined despite

declared reactivity of the antibody (Copps and White 2012, Garcia-Galiano et al. 2019). Consequently, an upregulation and thus activation of the IRS1-PI3K-AKT cascade can be assumed.

As Hinrichs et al. observed low serum IGF1 levels in *GHR*-KO pigs (Hinrichs et al. 2018) and IGF1 classically uses the IRS1-PI3K-AKT cascade via the IGF1R (Laviola et al. 2007), we expected a downregulation of this cascade. As opposed to this the IRS1-PI3K-AKT cascade was upregulated in *GHR*-KO pigs with the same pedigree and age. This can be explained by the activation of the IRS1 cascade by the INSR and/or the LEPR and not by the IGF1R, which is described in the hypothalamus (Niswender et al. 2004, Niswender and Schwartz 2003, Xu et al. 2005).

An upregulation via INSR may be possible, since an improvement in insulin sensitivity is described in GHRD human and mouse (Basu et al. 2018) and is also assumed in *GHR*-KO pigs (Hinrichs et al. 2018), but has to be evaluated on the hypothalamic-pituitary level by further studies using appropriate antibodies.

Because of higher serum leptin levels (Hinrichs et al. 2018), our findings of an increase in phosphorylated LEPR in hypothalami of *GHR*-KO pigs and IRS1 activation by LEPR described in the literature (Kwon et al. 2016, Park and Ahima 2014), an upregulation of IRS1-signaling via LEPR can be assumed.

As in hypothalami, phosphorylated IRS1 is also significantly higher in anterior pituitary glands of *GHR*-KO pigs. These findings and low serum IGF1 levels in *GHR*-KO pigs (Hinrichs et al. 2018) suggest that negative IGF1 feedback is not transduced via the IRS1-PI3K-AKT pathway neither in the hypothalamus nor in the anterior pituitary gland. In the literature it is described that the negative feedback of IGF1 on GH secretion in the pituitary gland is independent of IRS1-PI3K and mitogen-activated protein kinase (MAPK) but may be transferred via mTORC2 and AKT (Di Pasquale et al. 2018). Higher activity of AKT in hypothalami of *GHR*-KO pigs indicate that this theory is not suitable for negative IGF1 feedback in the hypothalamus. To evaluate this in pituitary glands, further investigations regarding mTOR and AKT will be helpful. Our data from non-targeted proteome analysis may give information on further players involved in this feedback cascade.

5.2. Unexpected findings in hypothalamic energy sensors (mTOR and AMPK)

Leptin and insulin play an important role in the regulation of energy homeostasis and food intake by the regulation of AMPK and mTOR in the hypothalamus (Hardie et al. 2012, Kwon et al. 2016, Park and Ahima 2014). Under physiological conditions their anorexigenic effect is transduced via the inhibition of orexigenic AMPK. In detail, the signaling of leptin via mTOR/S6K and of insulin via AKT and GSK3B inhibit the phosphorylation of AMPK at its catalytic α-subunit (Andersson et al. 2004, Jeon 2016, Kwon et al. 2016, Minokoshi et al. 2004, Park and Ahima 2014).

As opposed to the expected downregulation of orexigenic AMPK by the upregulation of the IRS1-PI3K-AKT cascade we observed no changes in mTOR and S6K, and even an increase in phosphorylation of AMPK in hypothalami of *GHR*-KO pigs compared to controls was revealed. This can only be explained by an unknown mechanism inhibiting anorexigenic signaling of leptin at the stage of mTOR/S6K and even converting it into an orexigenic signal by the upregulation of AMPK, leading to an “anti-leptin” effect.

It seems that the inactivation of AMPK and the connected inhibitory effect on food intake and bodyweight by leptin and/or insulin is not sufficient in *GHR*-KO pigs and a stimulus is even upregulating AMPK. This leads to orexigenic instead of anorexigenic signals from the hypothalamus and thus represents a state of caloric restriction instead of full energy stores like it is present in obese *GHR*-KO pigs.

The investigation of AMPK stimulatory agents like ghrelin, which is also a possible stimulator for GH release (Carreira et al. 2013) and our unpublished data from non-targeted proteome analysis may reveal underlying mechanisms (Hardie et al. 2012).

5.3. Protection against leptin insensitivity?

Despite these findings of controversial orexigenic and anorexigenic signals in hypothalami of *GHR*-KO pigs, leptin signaling via IRS1-PI3K-AKT seems to be intact. As reduced activity of this cascade is a sign for leptin insensitivity or even resistance due to high serum leptin levels in obesity (Cui et al. 2017, El-Haschimi et al. 2000, Liu

et al. 2018), this phenomenon could not be observed in our *GHR*-KO pigs. This leads to the hypothesis of a protective mechanism against obesity-associated leptin resistance in GHRD individuals, as it is described in the *Ecuadorian cohort* (Guevara-Aguirre et al. 2015).

To evaluate this model for LS regarding the underlying protective mechanism, further studies with age- and BMI-matched pigs would be a possible approach. Two possibilities seem to be suitable to explain the protection against leptin resistance: First, high GH or low IGF1 serum levels limit the rise of serum leptin levels like it is normally described in severe adiposity (Cui et al. 2017), and thus no leptin resistance can develop. Second, a hypothalamic GH/IGF1 dependent mechanism protects the leptin action from downregulation by permanently elevated leptin serum levels. For the option of a hypothalamic mechanism, leptin access to the hypothalamus as well as the improvement of the IRS1-PI3K-AKT cascade in hypothalamic neurons, as we investigated, may be responsible (Cui et al. 2017, El-Haschimi et al. 2000, Kwon et al. 2016, Liu et al. 2018). Also negative or positive regulators of leptin like suppressor of cytokine signaling 3 (SOCS3) and SH2B adapter protein 1 (SH2B1) may play a role in active LEPR-signaling despite high leptin levels of *GHR*-KO pigs (Zhou and Rui 2013).

In conclusion, our investigations revealed unexpected changes in hypothalamic leptin, insulin and IGF1 signaling of *GHR*-KO pigs and thus gave insight into regulatory alterations in *GHR*-KO pigs regarding the homeostatic regulation of energy balance and metabolism as well as protective aspects of GHRD. While anorexigenic signaling on the level of IRS1-PI3K-AKT seems to be normal in obese *GHR*-KO pigs, contrary orexigenic signals at the level of AMPK were determined. This leads to an uncertain understanding of regulatory units of energy homeostasis at the hypothalamic level and associated pathophysiological processes like leptin sensitivity. To give a clear picture of this eclectic regulation of the energy status at this central unit and embedding it into pathophysiological processes of GHRD, further research is necessary.

6. Summary

In individuals with Laron syndrome (LS), a rare autosomal recessive hereditary disease, the complex regulation of the somatotropic axis is disturbed by growth hormone receptor deficiency (GHRD). The resulting phenotype is characterized by reduced insulin-like growth factor 1 (IGF1) and high growth hormone (GH) serum concentrations as well as dwarfism, severe obesity, and increased insulin sensitivity. In order to evaluate the effects of this syndrome on central regulatory mechanisms of endocrine feedback-loops and metabolism, we investigated the activity of signaling cascades in hypothalami and anterior pituitaries of growth hormone receptor-knock out (*GHR*-KO) pigs. Therefore, we used sodium dodecyl sulfate–polyacrylamide gel electrophoresis (SDS-PAGE) and western immunoblotting techniques.

Despite low IGF1 serum levels, we observed an increased activity of insulin receptor substrate 1 (IRS1) related signaling in anterior pituitary and hypothalami of *GHR*-KO pigs. This suggests that negative IGF1 feedback on GH-production and -release from the periphery is not conveyed by this cascade. Instead this upregulation can be explained by the activation of the leptin receptor, which we have confirmed in hypothalami of *GHR*-KO pigs. Physiologically, an activation of IRS1 by leptin in the hypothalamus mediates an energy surplus and represents an intact communication of energy stores, while disorders leading to leptin insensitivity are pathologically related to obesity. In contrast to the intact activation of upper signaling, a typical “anti-hunger” effector, the mechanistic target of rapamycin (mTOR), was unchanged and its antagonist, adenosine monophosphate-activated protein kinase (AMPK), was even increased. This leads to an unclear picture of energy shortage and excess in a key regulator of the energy homeostasis of an obese organism associated with increased insulin sensitivity.

Since these results touch current research topics such as obesity-associated leptin resistance and GH/IGF1-feedback, further investigations using western blots as well as non-targeted proteome analyzes may be useful and are already being implemented.

7. Zusammenfassung

Bei Individuen mit Laron-Syndrom (LS), einer seltenen autosomal-rezessiven Erbkrankheit, ist die komplexe Regulation der Wachstumsachse durch eine Wachstumshormonrezeptordefizienz (GHRD) gestört. Der daraus entstehende Phänotyp resultiert aus erniedrigtem insulinähnlichen Wachstumsfaktor 1 (IGF1) bei gleichzeitig hohen Wachstumshormon (GH)-Serumkonzentrationen und ist durch Kleinwüchsigkeit und Fettleibigkeit, aber teilweise erhöhte Insulinsensitivität gekennzeichnet. Um die Auswirkungen dieses Syndroms auf zentrale Regelmechanismen von endokrinem Feedback und Metabolismus zu untersuchen, wurde die Aktivität entsprechender Signalkaskaden in Hypothalami und Adenohypophysen von *GHR*-knock out (*GHR*-KO) Schweinen untersucht. Hierfür wurden SDS-Polyacrylamid-Gelelektrophorese und Western Immunoblotting Methoden mit Meerrettichperoxidase konjugierten Antikörpern genutzt.

In Adenohypophysen und Hypothalami von *GHR*-KO-Schweinen wurde, trotz niedriger IGF1 Serumspiegel, eine erhöhte Aktivität von Insulinrezeptorsubstrat 1 (IRS1) oder der IRS1-Signalkaskade gefunden. Dies legt nahe, dass diese Kaskade nicht, wie in anderen Geweben, als Überträger der IGF1-Wirkung dient und somit das negative Feedback auf GH-Produktion und -Ausschüttung aus der Peripherie anderweitig übertragen wird. Stattdessen lässt sich die Aktivierung dieser Kaskade im Hypothalamus durch eine erhöhte Aktivierung des Leptinrezeptors in Zusammenhang mit erhöhten Leptinserumspiegeln begründen. Im gesunden Organismus vermittelt die Aktivierung dieser Kaskade durch Leptin im Hypothalamus einen Energieüberschuss und steht für eine intakte Kommunikation des Energiestatus. Störungen hingegen führen zu Leptininsensitivität und stehen im Zusammenhang mit Adipositas. Im Gegensatz zur Aktivität der oberen Signalwege, war ein typischer Effektor dieser „anti-Hunger“-Kaskade, das mechanistic target of rapamycin (mTOR), jedoch unverändert und ein Leptingegenspieler, Adenosinmonophosphat-aktivierte Proteinkinase (AMPK), sogar erhöht. Dies weist auf eine Entkopplung klassischer Wege der zellulären Wahrnehmung von Energiemangel und Energieüberschuss in einem zentralen

Regelzentrum der Energiehomöostase in einem durch Fettleibigkeit bei gleichzeitig erhöhter Insulinsensitivität gekennzeichneten Organismus hin.

Da diese Ergebnisse aktuelle Forschungsthemen wie Leptinresistenz in Zusammenhang mit Fettleibigkeit und GH-abhängigen Regelkreisen des Hypothalamus nur anschneiden, sind weitere Untersuchungen mittels Western Blots aber auch non-targeted Proteomanalysen mittels Massenspektrometrie sinnvoll und bereits in der Umsetzung.

8. Abbreviations

°C	degree Celsius
µg	microgram
µl	microliter
A	ampere
ACTH	adrenocorticotropic hormone
ADH / AVP	antidiuretic hormone / arginin-vasopression / vasopressin
AGRP	agouti-related peptide
AKT	protein kinase B
AMPK	5' adenosine monophosphate-activated protein kinase
ANOVA	analysis of variance
APS	aminocaproic acid
ARC	arcuate nucleus
BBB	blood-brain barrier
BCA	bicinchoninic acid solution
BMI	body mass index
BSA	bovine serum albumin (fraction V)
Cas9	CRISPR associated protein 9
CRH	corticotropin-releasing hormone
CRISPR	clustered regularly interspaced short palindromic repeats
CuSO4	copper(II)sulfate solution
DMH	dorsomedial hypothalamus
DSP	di-sodium hydrogen phosphate
E2	estradiol

EDTA	ethylenediaminetetraacetic acid
eIF4E	eukaryotic translation initiation factor 4
FDR	false discovery rate
F1	filial generation one
FOXO1	forkhead box protein O1
FSH	follicle stimulating hormone
GAPDH	glyceraldehyde 3-phosphate dehydrogenase
GH	growth hormone / somatotropin
GHR	human / porcine growth hormone receptor gene
Ghr	mouse growth hormone receptor gene
GHR	growth hormone receptor
GHRD	growth hormone receptor deficiency
GHRH	growth hormone-releasing hormone / somatoliberin
GHR-KO	growth hormone receptor-knockout (human / porcine)
Ghr-KO	growth hormone receptor-knockout (mouse)
GHRHR	growth hormone releasing hormone receptor
GNRH	gonadotropin-releasing hormone
GSK3B	glycogen synthase kinase 3 beta
HCl	hydrochloric acid
HP axis	hypothalamus pituitary axis
HRP	horseradish peroxidase
IGF1	insulin-like growth factor 1
IGF1R	insulin-like growth factor 1 receptor
IGFBP	IGF binding protein

INSR	insulin receptor
IRS1	insulin receptor substrate 1
JAK	janus kinase
KCl	potassium chloride
kD	kilodalton
KDP	potassium dihydrogen phosphate
LEPR	leptin receptor
LH	luteinizing hormone
LHT	lateral hypothalamus
LRb	long-form leptin receptor
LS	Laron syndrome
M	molar
MAPK	mitogen-activated protein kinase
mg	milligram
MJ	megajoule
ml	milliliter
mM	millimolar
mm	millimeter
mTOR	mechanistic target of rapamycin
mTORC	mechanistic target of rapamycin complex
NaCl	sodium chloride
NPY	neuropeptide Y
pAKT	phosphorylated AKT
pAMPK	phosphorylated AMPK

pGSK3B	phosphorylated pGSK3B
PI3K	phosphoinositide 3-kinase
pIRS1	phosphorylated IRS1
pLEPR	phosphrylated LEPR
pmTOR	phosphorylated mTOR
POMC	proopiomelanocortin
PPARG	peroxisome proliferator-activated receptor gamma
pPI3K	phosphorylated PI3K
Prog	progesterone
pS6K	phosphorylated S6K
PVN	paraventricular hypothalamic nucleus
RT	room temperature
S6K	ribosomal protein S6 kinase
SDS	sodium dodecyl sulfate
SDS-PAGE	sodium dodecyl sulfate polyacrylamide gel electrophoresis
SH2B1	SH2B adapter protein 1
SOCS3	suppressor of cytokine signaling 3
SST / SRIH	somatostatin / somatotropin release-inhibiting hormone
STAT3	signal transducer and activator of transcription 3
TBS	Tris-buffered saline solution
TBS-T	TBS with 0.1 % Tween20
Te	testosterone
TEMED	tetramethylethylenediamine
TRH	thyrotropin-releasing hormone

Tris	tris(hydroxymethyl)aminomethane
TSH	thyroid-stimulating hormone
V	volt
VMN	ventromedial hypothalamus
xg	gravitational force equivalent

9. Literature

Albl B, Haesner S, Braun-Reichhart C, Streckel E, Renner S, Seeliger F, Wolf E, Wanke R, Blutke A. 2016. Tissue Sampling Guides for Porcine Biomedical Models. Toxicologic pathology, 44(3): 414-420.

Amselem S, Duquesnoy P, Attree O, Novelli G, Bousnina S, Postel-Vinay MC, Goossens M. 1989. Laron dwarfism and mutations of the growth hormone-receptor gene. The New England journal of medicine, 321(15): 989-995.

Andersson U, Filipsson K, Abbott CR, Woods A, Smith K, Bloom SR, Carling D, Small CJ. 2004. AMP-activated protein kinase plays a role in the control of food intake. Journal of chemical biology, 279(13): 12005-12008.

Asa SL, Coschigano KT, Bellush L, Kopchick JJ, Ezzat S. 2000. Evidence for growth hormone (GH) autoregulation in pituitary somatotrophs in GH antagonist-transgenic mice and GH receptor-deficient mice. The American journal of pathology, 156(3): 1009-1015.

Bach LA. 2018. IGF-binding proteins. Journal of molecular endocrinology, 61(1): T11-t28.

Bailyes EM, Navé BT, Soos MA, Orr SR, Hayward AC, Siddle K. 1997. Insulin receptor/IGF-I receptor hybrids are widely distributed in mammalian tissues: quantification of individual receptor species by selective immunoprecipitation and immunoblotting. The Biochemical journal, 327(Pt 1): 209-215.

Baker J, Liu JP, Robertson EJ, Efstratiadis A. 1993. Role of insulin-like growth factors in embryonic and postnatal growth. Cell, 75(1): 73-82.

Banks WA, Kastin AJ, Huang W, Jaspan JB, Maness LM. 1996. Leptin enters the brain by a saturable system independent of insulin. Peptides, 17(2): 305-311.

Basu R, Qian Y, Kopchick JJ. 2018. MECHANISMS IN ENDOCRINOLOGY: Lessons from growth hormone receptor gene-disrupted mice: are there benefits of endocrine defects? European journal of endocrinology, 178(5): 155-181.

Beiki H, Liu H, Huang J, Manchanda N, Nonneman D, Smith TPL, Reecy JM, Tuggle CK. 2019. Improved annotation of the domestic pig genome through integration of Iso-Seq and RNA-seq data. BMC Genomics, 20(1): 344.

Bergan-Roller HE, Sheridan MA. 2018. The growth hormone signaling system: Insights into coordinating the anabolic and catabolic actions of growth hormone. General and comparative endocrinology, 258: 119-133.

Berryman DE, List EO, Sackmann-Sala L, Lubbers E, Munn R, Kopchick JJ. 2011. Growth hormone and adipose tissue: beyond the adipocyte. Growth hormone & IGF research : official journal of the Growth Hormone Research Society and the International IGF Research Society, 21(3): 113-123.

Carreira M, Crujeiras A, Andrade S, Monteiro M, Casanueva F. 2013. Ghrelin as a GH-releasing factor. Endocrine development, 25: 49-58.

Clarke IJ. 2015. Hypothalamus as an endocrine organ. Comprehensive Physiology, 5(1): 217-253.

Cocco C, Brancia C, Corda G, Ferri G-L. 2017. The Hypothalamic–Pituitary Axis and Autoantibody Related Disorders. International journal of molecular sciences, 18(11): 2322.

Considine RV, Sinha MK, Heiman ML, Kriauciunas A, Stephens TW, Nyce MR, Ohannesian JP, Marco CC, McKee LJ, Bauer TL, Caro JF. 1996. Serum immunoreactive-leptin concentrations in normal-weight and obese humans. The New England journal of medicine, 334(5): 292-295.

Copps KD, White MF. 2012. Regulation of insulin sensitivity by serine/threonine phosphorylation of insulin receptor substrate proteins IRS1 and IRS2. Diabetologia, 55(10): 2565-2582.

Coschigano KT, Clemmons D, Bellush LL, Kopchick JJ. 2000. Assessment of growth parameters and life span of GHR/BP gene-disrupted mice. Endocrinology, 141(7): 2608-2613.

Cota D, Proulx K, Smith KAB, Kozma SC, Thomas G, Woods SC, Seeley RJ. 2006. Hypothalamic mTOR signaling regulates food intake. Science, 312(5775): 927-930.

Cui H, López M, Rahmouni K. 2017. The cellular and molecular bases of leptin and ghrelin resistance in obesity. Nature reviews. Endocrinology, 13(6): 338-351.

de Graauw M, Hensbergen P, van de Water B. 2006. Phospho-proteomic analysis of cellular signaling. Electrophoresis, 27(13): 2676-2686.

Di Pasquale C, Gentilin E, Falletta S, Bellio M, Buratto M, Degli Uberti E, Chiara Zatelli M. 2018. PI3K/Akt/mTOR pathway involvement in regulating growth hormone secretion in a rat pituitary adenoma cell line. Endocrine, 60(2): 308-316.

El-Haschimi K, Pierroz DD, Hileman SM, Bjørbaek C, Flier JS. 2000. Two defects contribute to hypothalamic leptin resistance in mice with diet-induced obesity. The Journal of clinical investigation, 105(12): 1827-1832.

Eshet R, Laron Z, Pertzelan A, Arnon R, Dintzman M. 1984. Defect of human growth hormone receptors in the liver of two patients with Laron-type dwarfism. Israel journal of medical sciences, 20(1): 8-11.

Fei H, Okano HJ, Li C, Lee GH, Zhao C, Darnell R, Friedman JM. 1997. Anatomic localization of alternatively spliced leptin receptors (Ob-R) in mouse brain and other tissues. Proceedings of the National Academy of Sciences of the United States of America, 94(13): 7001-7005.

Friedman JM, Halaas JL. 1998. Leptin and the regulation of body weight in mammals. Nature, 395(6704): 763-770.

Gao Q, Wolfgang MJ, Neschen S, Morino K, Horvath TL, Shulman GI, Fu XY. 2004. Disruption of neural signal transducer and activator of transcription 3 causes obesity, diabetes, infertility, and thermal dysregulation. Proceedings of the National Academy of Sciences of the United States of America, 101(13): 4661-4666.

Garcia-Galiano D, Borges BC, Allen SJ, Elias CF. 2019. PI3K signalling in leptin receptor cells: Role in growth and reproduction. Journal of neuroendocrinology, 31(5): e12685.

Giustina A, Veldhuis JD. 1998. Pathophysiology of the neuroregulation of growth hormone secretion in experimental animals and the human. Endocrine reviews, 19(6): 717-797.

Godowski PJ, Leung DW, Meacham LR, Galgani JP, Hellmiss R, Keret R, Rotwein PS, Parks JS, Laron Z, Wood WI. 1989. Characterization of the human growth hormone receptor gene and demonstration of a partial gene deletion in two patients with Laron-type dwarfism. Proceedings of the National Academy of Sciences of the United States of America, 86(20): 8083-8087.

Guevara-Aguirre J, Balasubramanian P, Guevara-Aguirre M, Wei M, Madia F, Cheng CW, Hwang D, Martin-Montalvo A, Saavedra J, Ingles S, de Cabo R, Cohen P, Longo VD. 2011. Growth hormone receptor deficiency is associated with a major reduction in pro-aging signaling, cancer, and diabetes in humans. Science translational medicine, 3(70): 70ra13.

Guevara-Aguirre J, Rosenbloom AL, Balasubramanian P, Teran E, Guevara-Aguirre M, Guevara C, Procel P, Alfaras I, De Cabo R, Di Biase S, Narvaez L, Saavedra J, Longo VD. 2015. GH Receptor Deficiency in Ecuadorian Adults Is Associated With Obesity and Enhanced Insulin Sensitivity. The Journal of clinical endocrinology and metabolism, 100(7): 2589-2596.

Guo XH, Zhao NM, Chen SH, Teixeira J. 1990. Small-angle neutron scattering study of the structure of protein/detergent complexes. Biopolymers, 29(2): 335-346.

Hardie DG, Ross FA, Hawley SA. 2012. AMPK: a nutrient and energy sensor that maintains energy homeostasis. Nature reviews. Molecular cell biology, 13(4): 251-262.

Hetz JA, Menzies BR, Shaw G, Rao A, Clarke IJ, Renfree MB. 2015. Growth axis maturation is linked to nutrition, growth and developmental rate. Molecular and cellular endocrinology, 411: 38-48.

Hinrichs A, Kessler B, Kurome M, Blutke A, Kemter E, Bernau M, Scholz AM, Rathkolb B, Renner S, Bultmann S, Leonhardt H, Hrabě de Angelis M, Nagashima H, Hoeflich A, Blum WF, Bidlingmaier M, Wanke R, Dahlhoff M, Wolf E. 2018. Growth hormone receptor-deficient pigs resemble the pathophysiology of human Laron syndrome and reveal altered activation of signaling cascades in the liver. Molecular metabolism, 11: 113-128.

Isaksson OG, Lindahl A, Nilsson A, Isgaard J. 1987. Mechanism of the stimulatory effect of growth hormone on longitudinal bone growth. Endocrine reviews, 8(4): 426-438.

Jeon SM. 2016. Regulation and function of AMPK in physiology and diseases. Experimental & molecular medicine, 48(7): e245.

Kaplan SA, Cohen P. 2007. The somatomedin hypothesis 2007: 50 years later. The Journal of clinical endocrinology and metabolism, 92(12): 4529-4535.

Keenan DM, Veldhuis JD. 2016. Pulsatility of hypothalamo-pituitary hormones: a challenge in quantification. Physiology (Bethesda, Md.), 31(1): 34-50.

Kleinridders A, Könner AC, Brüning JC. 2009. CNS-targets in control of energy and glucose homeostasis. Current opinion in pharmacology, 9(6): 794-804.

Kopchick JJ. 2003. History and future of growth hormone research. Hormone research, 60 Suppl 3: 103-112.

Kopchick JJ, Bellush LL, Coschigano KT. 1999. Transgenic models of growth hormone action. Annual review of nutrition, 19: 437-461.

Kwon O, Kim KW, Kim MS. 2016. Leptin signalling pathways in hypothalamic neurons. Cellular and molecular life sciences : CMLS, 73(7): 1457-1477.

Laemmli UK. 1970. Cleavage of structural proteins during the assembly of the head of bacteriophage T4. Nature, 227(5259): 680-685.

Laron Z. 2004. IGF-1 and insulin as growth hormones. Novartis Foundation symposium, 262: 56-77; discussion 77-83, 265-268.

Laron Z. 2008. The GH-IGF1 axis and longevity. The paradigm of IGF1 deficiency. Hormones (Athens), 7(1): 24-27.

Laron Z, Avitzur Y, Klinger B. 1995. Carbohydrate metabolism in primary growth hormone resistance (Laron syndrome) before and during insulin-like growth factor-I treatment. Metabolism: clinical and experimental, 44(10 Suppl 4): 113-118.

Laron Z, Kauli R, Lapkina L, Werner H. 2017. IGF-I deficiency, longevity and cancer protection of patients with Laron syndrome. Mutation research. Reviews in mutation research, 772: 123-133.

Laron Z, Klinger B. 1994. Laron syndrome: clinical features, molecular pathology and treatment. Hormone research, 42(4-5): 198-202.

Laron Z, Kopchick JJ. 2011. Laron Syndrome - From Man to Mouse. Heidelberg: Springer.

Laron Z, Pertzelan A, Mannheimer S. 1966. Genetic pituitary dwarfism with high serum concentation of growth hormone--a new inborn error of metabolism? Israel journal of medical sciences, 2(2): 152-155.

Laviola L, Natalicchio A, Giorgino F. 2007. The IGF-I signaling pathway. Current pharmaceutical design, 13(7): 663-669.

Le Roith D, Scavo L, Butler A. 2001. What is the role of circulating IGF-I? Trends in endocrinology and metabolism : TEM, 12(2): 48-52.

Leng G, Pineda R, Sabatier N, Ludwig M. 2015. 60 YEARS OF NEUROENDOCRINOLOGY: The posterior pituitary, from Geoffrey Harris to our present understanding. The Journal of endocrinology, 226(2): T173-185.

List EO, Sackmann-Sala L, Berryman DE, Funk K, Kelder B, Gosney ES, Okada S, Ding J, Cruz-Topete D, Kopchick JJ. 2011. Endocrine parameters and phenotypes of the growth hormone receptor gene disrupted (GHR-/-) mouse. Endocrine reviews, 32(3): 356-386.

Liu J, Yang X, Yu S, Zheng R. 2018. The Leptin Resistance. Advances in experimental medicine and biology, 1090: 145-163.

Liu JL, Coschigano KT, Robertson K, Lipsett M, Guo Y, Kopchick JJ, Kumar U, Liu YL. 2004. Disruption of growth hormone receptor gene causes diminished pancreatic islet size and increased insulin sensitivity in mice. American journal of physiology. Endocrinology and metabolism, 287(3): E405-413.

Maffei M, Halaas J, Ravussin E, Pratley RE, Lee GH, Zhang Y, Fei H, Kim S, Lallone R, Ranganathan S, Kern PA, Friedman JM. 1995. Leptin levels in human and rodent: measurement of plasma leptin and ob RNA in obese and weight-reduced subjects. Nature medicine, 1(11): 1155-1161.

Masternak MM, Bartke A, Wang F, Spong A, Gesing A, Fang Y, Salmon AB, Hughes LF, Liberati T, Boparai R, Kopchick JJ, Westbrook R. 2012. Metabolic effects of intra-abdominal fat in GHRKO mice. Aging Cell, 11(1): 73-81.

Masuzaki H, Ogawa Y, Isse N, Satoh-Asahara N, Okazaki T, Shigemoto M, Mori K, Tamura N, Hosoda K, Yoshimasa Y. 1995. Human Obese Gene Expression: Adipocyte-Specific Expression and Regional Differences in the Adipose Tissue. Diabetes, 44: 855-858.

Mercer JG, Hoggard N, Williams LM, Lawrence CB, Hannah LT, Trayhurn P. 1996. Localization of leptin receptor mRNA and the long form splice variant (Ob-Rb) in mouse hypothalamus and adjacent brain regions by in situ hybridization. FEBS letters, 387(2-3): 113-116.

Minokoshi Y, Alquier T, Furukawa N, Kim YB, Lee A, Xue B, Mu J, Foufelle F, Ferré P, Birnbaum MJ, Stuck BJ, Kahn BB. 2004. AMP-kinase regulates food intake by responding to hormonal and nutrient signals in the hypothalamus. Nature, 428(6982): 569-574.

Mukherji M. 2005. Phosphoproteomics in analyzing signaling pathways. Expert review of proteomics, 2(1): 117-128.

Myers MG, Cowley MA, Münzberg H. 2008. Mechanisms of leptin action and leptin resistance. Annual review of physiology, 70: 537-556.

Niswender KD, Baskin DG, Schwartz MW. 2004. Insulin and its evolving partnership with leptin in the hypothalamic control of energy homeostasis. Trends in endocrinology and metabolism : TEM, 15(8): 362-369.

Niswender KD, Schwartz MW. 2003. Insulin and leptin revisited: adiposity signals with overlapping physiological and intracellular signaling capabilities. Frontiers in neuroendocrinology, 24(1): 1-10.

Pandini G, Frasca F, Mineo R, Sciacca L, Vigneri R, Belfiore A. 2002. Insulin/insulin-like growth factor I hybrid receptors have different biological characteristics depending on the insulin receptor isoform involved. The Journal of biological chemistry, 277(42): 39684-39695.

Park HK, Ahima RS. 2014. Leptin signaling. F1000prime reports, 6: 73.

Pedrini MT, Giorgino F, Smith RJ. 1994. cDNA cloning of the rat IGF I receptors: structural analysis of rat and human IGF I and insulin receptors reveals differences in alternative splicing and receptor-specific domain conservation. Biochemical and biophysical research communications, 202(2): 1038-1046.

Peng X-D, Park S, Gadelha MR, Coschigano KT, Kopchick JJ, Frohman LA, Kineman RD. 2001. The growth hormone (GH)-axis of GH receptor/binding protein gene-disrupted and metallothionein-human GH-releasing hormone transgenic mice: hypothalamic neuropeptide and pituitary receptor expression in the absence and presence of GH feedback. Endocrinology, 142(3): 1117-1123.

Rajaram S, Baylink DJ, Mohan S. 1997. Insulin-like growth factor-binding proteins in serum and other biological fluids: regulation and functions. Endocrine reviews, 18(6): 801-831.

Reinders J, Sickmann A. 2005. State-of-the-art in phosphoproteomics. Proteomics, 5(16): 4052-4061.

Riedel EO, Hinrichs A, Kemter E, Dahlhoff M, Backman M, Rathkolb B, Prehn C, Adamski J, Renner S, Blutke A, Hrabě de Angelis M, Bidlingmaier M, Schopohl J, Arnold GJ, Fröhlich T, Wolf E. 2020. Functional changes of the liver in the absence of growth hormone (GH) action–proteomic and metabolomic insights from a GH receptor deficient pig model. Molecular metabolism, 36: 100978.

Roh E, Kim MS. 2016. Brain Regulation of Energy Metabolism. Endocrinology and metabolism (Seoul, Korea), 31(4): 519-524.

Romero CJ, Ng Y, Luque RM, Kineman RD, Koch L, Bruning JC, Radovick S. 2010. Targeted deletion of somatotroph insulin-like growth factor-I signaling in a cell-specific knockout mouse model. Molecular endocrinology (Baltimore, Md.), 24(5): 1077-1089.

Rosenbaum M, Nicolson M, Hirsch J, Heymsfield SB, Gallagher D, Chu F, Leibel RL. 1996. Effects of gender, body composition, and menopause on plasma concentrations of leptin. The Journal of clinical endocrinology and metabolism, 81(9): 3424-3427.

Rosenbloom AL, Guevara-Aguirre J. 1998. Lessons from the genetics of laron syndrome. Trends in endocrinology and metabolism : TEM, 9(7): 276-283.

Rosenbloom AL, Guevara-Aguirre J, Berg MA, Francke U. 1998. Stature in Ecuadorians heterozygous for growth hormone receptor gene E180 splice mutation does not differ from that of homozygous normal relatives. The Journal of clinical endocrinology and metabolism, 83(7): 2373-2375.

Rosenfeld RG, Rosenbloom AL, Guevara-Aguirre J. 1994. Growth hormone (GH) insensitivity due to primary GH receptor deficiency. Endocrine reviews, 15(3): 369-390.

Russell WMS, Burch RL. 1959. The Principles of Humane Experimental Technique. London: Methuen Publishing.

Sam S, Frohman LA. 2008. Normal physiology of hypothalamic pituitary regulation. Endocrinology and metabolism clinics of North America, 37(1): 1-22, vii.

Shevah O, Laron Z. 2007. Patients with congenital deficiency of IGF-I seem protected from the development of malignancies: a preliminary report. Growth hormone & IGF research : official journal of the Growth Hormone Research Society and the International IGF Research Society, 17(1): 54-57.

Smith PK, Krohn RI, Hermanson GT, Mallia AK, Gartner FH, Provenzano MD, Fujimoto EK, Goeke NM, Olson BJ, Klenk DC. 1985. Measurement of protein using bicinchoninic acid. Analytical biochemistry, 150(1): 76-85.

Summers KM, Bush SJ, Wu C, Su AI, Muriuki C, Clark EL, Finlayson HA, Eory L, Waddell LA, Talbot R, Archibald AL, Hume DA. 2020. Functional Annotation of the Transcriptome of the Pig, Sus scrofa, Based Upon Network Analysis of an RNAseq Transcriptional Atlas. Frontiers in genetics, 10: 1355.

Towbin H, Staehelin T, Gordon J. 1979. Electrophoretic transfer of proteins from polyacrylamide gels to nitrocellulose sheets: procedure and some applications. Proceedings of the National Academy of Sciences of the United States of America, 76(9): 4350-4354.

Varela-Nieto I, Chowen JA. 2005. The growth hormone/insulin-like growth factor axis during development. New York: Springer.

Walker JM. 1994. The bicinchoninic acid (BCA) assay for protein quantitation. Methods in molecular biology (Clifton, N.J.), 32: 5-8.

Waterson MJ, Horvath TL. 2015. Neuronal Regulation of Energy Homeostasis: Beyond the Hypothalamus and Feeding. Cell metabolism, 22(6): 962-970.

Weber K, Osborn M. 1969. The reliability of molecular weight determinations by dodecyl sulfate-polyacrylamide gel electrophoresis. The Journal of biological chemistry, 244(16): 4406-4412.

Winogradoff D, John S, Aksimentiev A. 2020. Protein unfolding by SDS: the microscopic mechanisms and the properties of the SDS-protein assembly. Nanoscale, 12(9): 5422-5434.

Xu AW, Kaelin CB, Takeda K, Akira S, Schwartz MW, Barsh GS. 2005. PI3K integrates the action of insulin and leptin on hypothalamic neurons. The Journal of clinical investigation, 115(4): 951-958.

Zhang Y, Proenca R, Maffei M, Barone M, Leopold L, Friedman JM. 1994. Positional cloning of the mouse obese gene and its human homologue. Nature, 372(6505): 425-432.

Zhou Y, Rui L. 2013. Leptin signaling and leptin resistance. Frontiers of medicine, 7(2): 207-222.

Zhou Y, Xu BC, Maheshwari HG, He L, Reed M, Lozykowski M, Okada S, Cataldo L, Coschigamo K, Wagner TE, Baumann G, Kopchick JJ. 1997. A mammalian model for Laron syndrome produced by targeted disruption of the mouse growth hormone receptor/binding protein gene (the Laron mouse). Proceedings of the National Academy of Sciences of the United States of America, 94(24): 13215-13220.

10. List of figures and tables

Acknowledgement

First of all, I would like to thank Prof. Eckhard Wolf for providing me the opportunity to carry out this work at the chair for Molecular Animal Breeding and Biotechnology, Gene Center, Ludwig-Maximilians-Universität Munich, and Prof. Mathias Müller for supporting this thesis at the Vetmeduni Vienna. It was an extraordinary opportunity for a diploma thesis!

Special thanks to my mentor Dr. Arne Hinrichs, for spending immense time and patience to support my work and creating a pleasant working atmosphere. I am really looking forward to working together at the Moorversuchsgut!

I am particularly thankful to Dr. Elisabeth Kemter and Dr. Christine Hösl for their support in all technical and helpful advices in scientific questions.

I also would like to thank Franziska Kress (Gene Center LMU) for her technical assistance in the laboratory and Dr. Alexander Tichy (Vetmeduni Vienna) for his support regarding statistical analysis.

And finally, a heartfelt “THANK YOU” to my parents for their indefatigable support and encouragement at all time!